AD A050961

(1)
B.S.

MARINE PHYSICAL LABORATORY
of the Scripps Institution of Oceanography
San Diego, California 92152

A COMPARISON BETWEEN ACOUSTIC REVERBERATION STRUCTURES AT 87.5 kHz AND INTERNAL WAVES

G. T. Kaye

AD No. ____
DDC FILE COPY

Sponsored by the
Advanced Research Projects Agency
ARPA Code Number 2127 and Program Code Number 7D40
and
the Office of Naval Research
Contract N00014-75-C-0349

Reproduction in whole or in part is permitted
for any purpose of the U. S. Government

Document cleared for public release
and sale; its distribution is unlimited.

17 October 1977

DDC
RECEIVED
MAR 9 1978
B

SIO REFERENCE 77-24

UNIVERSITY OF CALIFORNIA, SAN DIEGO
MARINE PHYSICAL LABORATORY OF THE
SCRIPPS INSTITUTION OF OCEANOGRAPHY
SAN DIEGO, CALIFORNIA 92152

A COMPARISON BETWEEN ACOUSTIC REVERBERATION STRUCTURES AT 87.5 kHz AND INTERNAL WAVES

G. T. Kaye

Sponsored by the
Advanced Research Projects Agency
ARPA Code Number 2127 and Program Code Number 7D40
and
the Office of Naval Research
Contract N00014-75-C-0549

SIO REFERENCE 77-24

17 October 1977

Reproduction in whole or in part is permitted
for any purpose of the U. S. Government

Document cleared for public release
and sale; its distribution is unlimited.

F. N. Spiess

F. N. SPIESS, DIRECTOR
MARINE PHYSICAL LABORATORY

DDC
RECEIVED
MAR 9 1978
B

MPL-U-85/77

SECURITY CLASSIFICATION OF THIS PAGE (When Data Entered)

REPORT DOCUMENTATION PAGE

READ INSTRUCTIONS BEFORE COMPLETING FORM

1. REPORT NUMBER: SIO REFERENCE 77-24
2. GOVT ACCESSION NO.
3. RECIPIENT'S CATALOG NUMBER

4. TITLE (and Subtitle): A COMPARISON BETWEEN ACOUSTIC REVERBERATION STRUCTURES AT 87.5 kHz AND INTERNAL WAVES.

5. TYPE OF REPORT & PERIOD COVERED: FINAL REPORT.

6. PERFORMING ORG. REPORT NUMBER: MPL-U-85/77, SIO-Ref-77-24

7. AUTHOR(s): G. T. Kaye

8. CONTRACT OR GRANT NUMBER(s): ARPA Code 2127 and Program Code 7D40 and ONR N00014-75-C-0549 new

9. PERFORMING ORGANIZATION NAME AND ADDRESS: University of California, San Diego, Marine Physical Laboratory of the Scripps Institution of Oceanography, San Diego, California 92152

10. PROGRAM ELEMENT, PROJECT, TASK AREA & WORK UNIT NUMBERS: N00014-75-C-0749, ARPA Order-2127

11. CONTROLLING OFFICE NAME AND ADDRESS: Office of Naval Research, Code 222, Department of the Navy, Arlington, Virginia 22217

12. REPORT DATE: 17 October 1977

13. NUMBER OF PAGES: 30 (34p.)

14. MONITORING AGENCY NAME & ADDRESS (if different from Controlling Office)

15. SECURITY CLASS. (of this report)

15a. DECLASSIFICATION/DOWNGRADING SCHEDULE

16. DISTRIBUTION STATEMENT (of this Report)

Document cleared for public release and sale; its distribution is unlimited.

17. DISTRIBUTION STATEMENT (of the abstract entered in Block 20, if different from Report)

18. SUPPLEMENTARY NOTES

19. KEY WORDS (Continue on reverse side if necessary and identify by block number)

Acoustic reverberation data, 87.5 kHz, narrow-beam echo sounder, southern California, backscattering analysis, discrete point scatterers.

20. ABSTRACT (Continue on reverse side if necessary and identify by block number)

Reverberation data at 87.5 kHz were obtained with a narrow-beam echo sounder from R/P FLIP in January and June 1977 off southern California. Analysis of these data shows that backscattering below the wind-mixed layer was due primarily to discrete point scatterers, which had target strengths ranging from -38 to -73 dB and densities of 0.05 to 50 individuals per 1000 m^3. Based upon these characteristics, the identities of the scatterers are probably swimbladder fish, and possibly squid and siphonophores. Backscattering from smaller organisms has been observed as patches or as a limited number of

DD FORM 1 JAN 73 1473 EDITION OF 1 NOV 65 IS OBSOLETE S/N 0102-LF-014-6601

SECURITY CLASSIFICATION OF THIS PAGE (When Data Entered)

217 400

scattering layers. A visual comparison between scatterer motions and isotherm depth fluctuations showed excellent correlation in terms of both phase and amplitude. Minimum total wave amplitudes as small as three meters were observed. It is suggested that this depth resolution might be improved with better data processing techniques and increased system performance.

ACCESSION for
NTIS White Section
DDC Buff Section
UNANNOUNCED
JUSTIFICATION
BY
DISTRIBUTION/AVAILABILITY CODES
Dist. AVAIL. and/or SPECIAL
A

A COMPARISON BETWEEN ACOUSTIC REVERBERATION STRUCTURES AT 87.5 kHz AND INTERNAL WAVES

G. T. Kaye

University of California, San Diego
Marine Physical Laboratory
Scripps Institution of Oceanography
San Diego, California 92152

Abstract

Reverberation data at 87.5 kHz were obtained with a narrow-beam echo sounder from R/P FLIP in January and June 1977 off southern California. Analysis of these data shows that backscattering below the wind-mixed layer was due primarily to discrete point scatterers, which had target strengths ranging from -38 to -73 dB_3 and densities of 0.05 to 50 individuals per 1000 m^3. Based upon these characteristics, the identities of the scatterers are probably swimbladder fish, and possibly squid and siphonophores. Backscattering from smaller organisms has been observed as patches or as a limited number of scattering layers. A visual comparison between scatterer motions and isotherm depth fluctuations showed excellent correlation in terms of both phase and amplitude. Minimum total wave amplitudes as small as three meters were observed. It is suggested that this depth resolution might be improved with better data processing techniques and increased system performance.

INTRODUCTION

The use of acoustic techniques to study internal waves requires an understanding of the scatterers that produce the reverberation data. One is concerned with inferring from the backscattering information the occurrence of short time-scale mixing and internal wave activity. Prerequisites for these inferences are identification of the backscatterers and an evaluation of how well an individual scatterer mimics the motion of a water parcel.

In this context it is suggested that the scatterers should have the following ideal properties:

(1) they should be abundant within at least the first 250 m of the water column;

(2) they should be sufficiently dense so that a narrow-beam system can identify and track a small volume;

(3) the scatterers should be distributed homogeneously in the horizontal dimension to avoid patchiness and, therefore, "holidays" in the data record;

(4) they should have a wide geographical range so that the system will be viable in all oceanic provinces;

(5) the scatterers should be neutrally buoyant with minimal self-propulsion so that they will be dependable tracers of water motion.

BACKGROUND

The MPL 87.5 kHz echo sounder is described in detail in Squier, et al. (1976). Eight transducers are driven in parallel to produce a source level of 227 dB//μ Pa. They form a 1° ($\pm\frac{1}{2}^{\circ}$ at 3 dB down) acoustic beam. The first sidelobe of the directivity pattern is 2° from the acoustic axis and is 6 dB down from the main lobe. The single receiving element, which is not

one of the transmitting elements, has a sensitivity of -176 dB//μ Pa; the 3 dB down point of the receiver pattern is at $4\frac{1}{2}^{o}$. The nearfield of the echo sounder is approximately 50 m. Pulse durations as short as 0.1 msec have been used.

This instrument was originally intended to observe small-scale bottom topography from R/P FLIP. During testing, backscatter from within the 400 m of the water column immediately below FLIP was observed. High-frequency ($\sim$ 3 cph) internal wave type motions were observed with amplitudes as great as 10 m and with vertical coherences as great as 100 m.

SCATTERER CHARACTERISTICS

Initially the scattering was interpreted as reflections from sound velocity microstructure and the results were reported in terms of reflection coefficients (Fisher and Squier, 1975). Subsequent work has shown that the backscattering is due to point scatterers, since the reflection coefficients did not vary as the echo sounder orientation was varied. We can expect that microstructure will have orientations no more than a few degrees from horizontal. Because of this we would expect that backscattering from microstructure reflectors would fall off rapidly as the angle of incidence varies from normal to the density layering to off-normal. Squier, et al. (1976) report no change in backscatter between a vertical orientation of the echo sounder and an orientation of 30^{o} off from vertical. This can be seen qualitatively in Figure 1 from data taken in June 1977. The echo sounder was rotated over a 30-min period from 270^{o} (horizontal) through 180^{o} (vertically-downward) to 090^{o} (horizontal). The change in slant range to scatterers at a fixed depth gives the appearance of vertical migration in this presentation. At 180^{o} a surface return from the backlobe of the echo sounder is seen at 170 m. If reflections from microstructure were significant, we would expect to observe increased backscatter in this orientation; however, such an increase is not apparent.

A sample of the data taken in January 1977 at position 31^{o}N 120^{o}W is shown in Figure 2. The pulse duration was 0.6 msec and the pulse repetition rate was once per second. This data presentation is different from the first figure in that the record was constructed from digitized data, while the first figure was made on an analog recorder with some time-varying-gain. The digitized data have been shaded according to target strength. Compensation for transmission loss was according to a two-way scattering (40 log R) with an attenuation coefficient of 21 dB/km (Fisher and Simmons, 1977). Target strengths were calculated relative to an ideal sphere of a radius 2 m. Because the echo sounder was mounted at the 60 m depth on FLIP, backscatter from the hull and sea surface partially masked the data in the upper portion of the record. An attempt has been made to compensate for this interference by subtracting a mean scattering level from the data in this region. Although the subtraction allows a qualitative presentation of the data, target strength information in the interference region was not used.

This is the densest scatterer concentration that was noted during the observation period of $22\frac{1}{2}$ hr. In spite of this concentration the scatterers appear to be discrete. The faint scattering layer at 400 m is real and persisted throughout most of the record. A thin scattering layer is observed around 70 m which corresponded to the top of the thermocline. The temperature profile for this time showed that the well-mixed layer extended to a depth near 60 m. Between 60 and 70 m there was a sharp decrease from 15.5 to 12^{o}C. Below 70 m the temperature dropped off smoothly to 6.5^{o} at 400 m. Apparent wave activity is noted around 200 m between 0100 and 0200. Between 200 and 250 m there is a dramatic change in the reverberation at 0210. This could be due to either patchiness in the scatterer distribution or to a change in the acoustic strength of the scatterers. Similar abrupt changes have been seen in other records during times of vertical migration (Fisher, personal communication). A vertical migration commenced around midnight that corresponded with the passage of rain squalls, which apparently triggered a downward migration from the mixed layer to depths of 100-250 m. Prior to the squalls the sky had been clear with a full moon. After the squall passed around 0230, the sky cleared and the moon had not set. Some of the scatterers continued their downward migration and others returned to the mixed layer.

To display the data in greater detail, portions of this record were plotted in expanded form in Figures 3a and 3b. In these we can see that the scattering structure presented in Figure 2 is resolvable as point scatterers which are discrete and mobile with vertical swim speeds as great as 8 cm/sec. Interpretation of the wave activity as internal waves is speculative at this point without additional measurements, since the vertical velocities of individual scatterers are greater than typical internal wave vertical velocities. Although the data in this time period are atypical of most of the data as seen by this observer and by Fisher, they do point out a difficulty in interpreting scatterer motion as water motion.

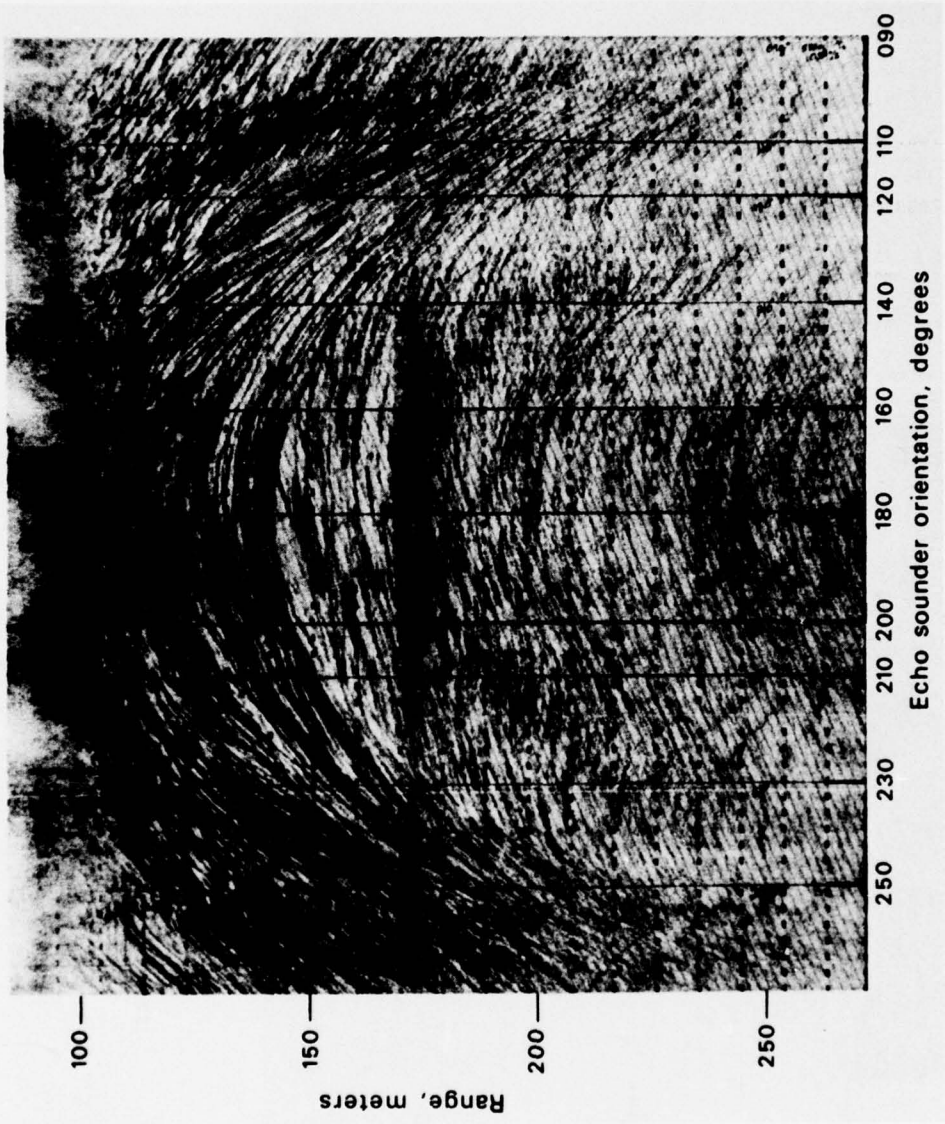

Figure 1. Variation of acoustic backscatter with echo sounder orientation. 270° and 090° are horizontal orientations and 180° is vertically downward.

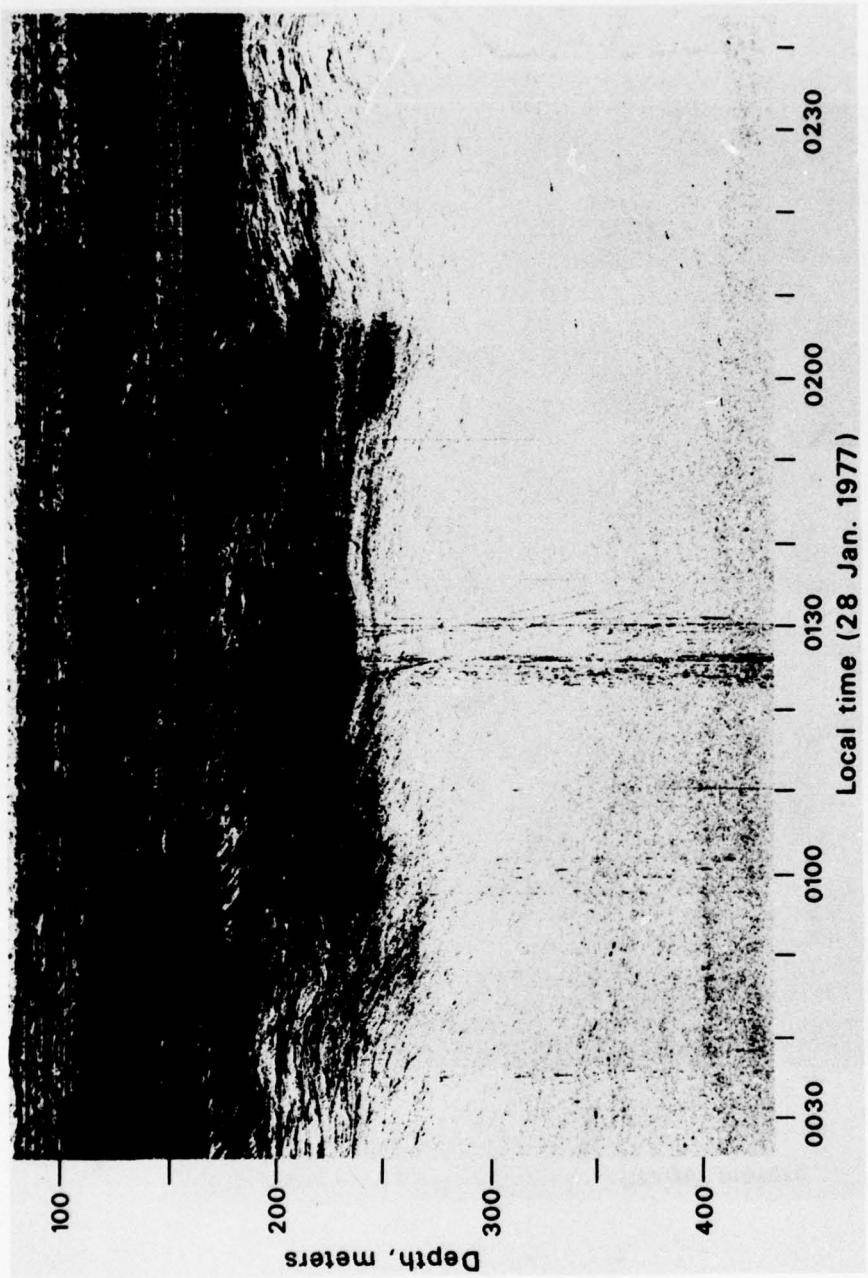

Figure 2. Target strength record constructed from digitized data. Internal wave type motions are seen around 200 m and between 0100 and 0150.

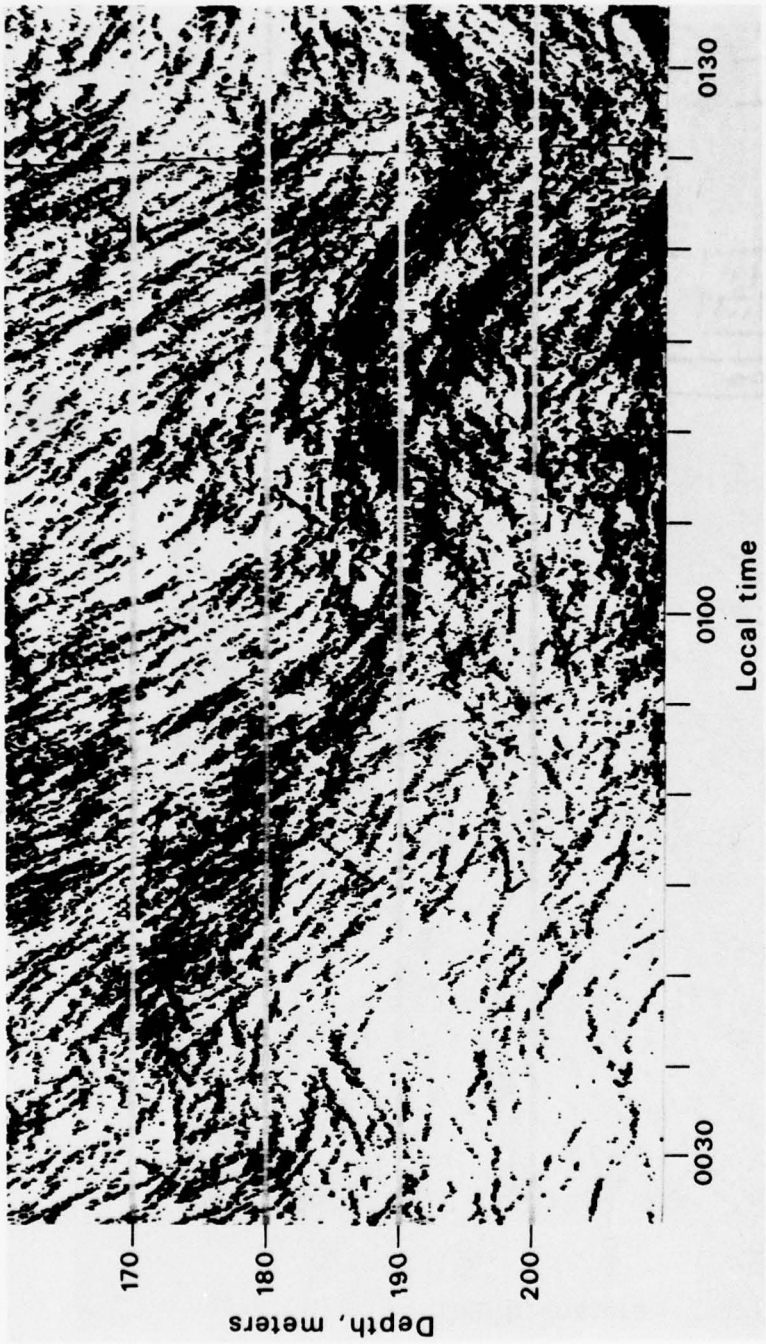

Figure 3a. Enlarged target strength record showing discrete scatterers and wave motion.

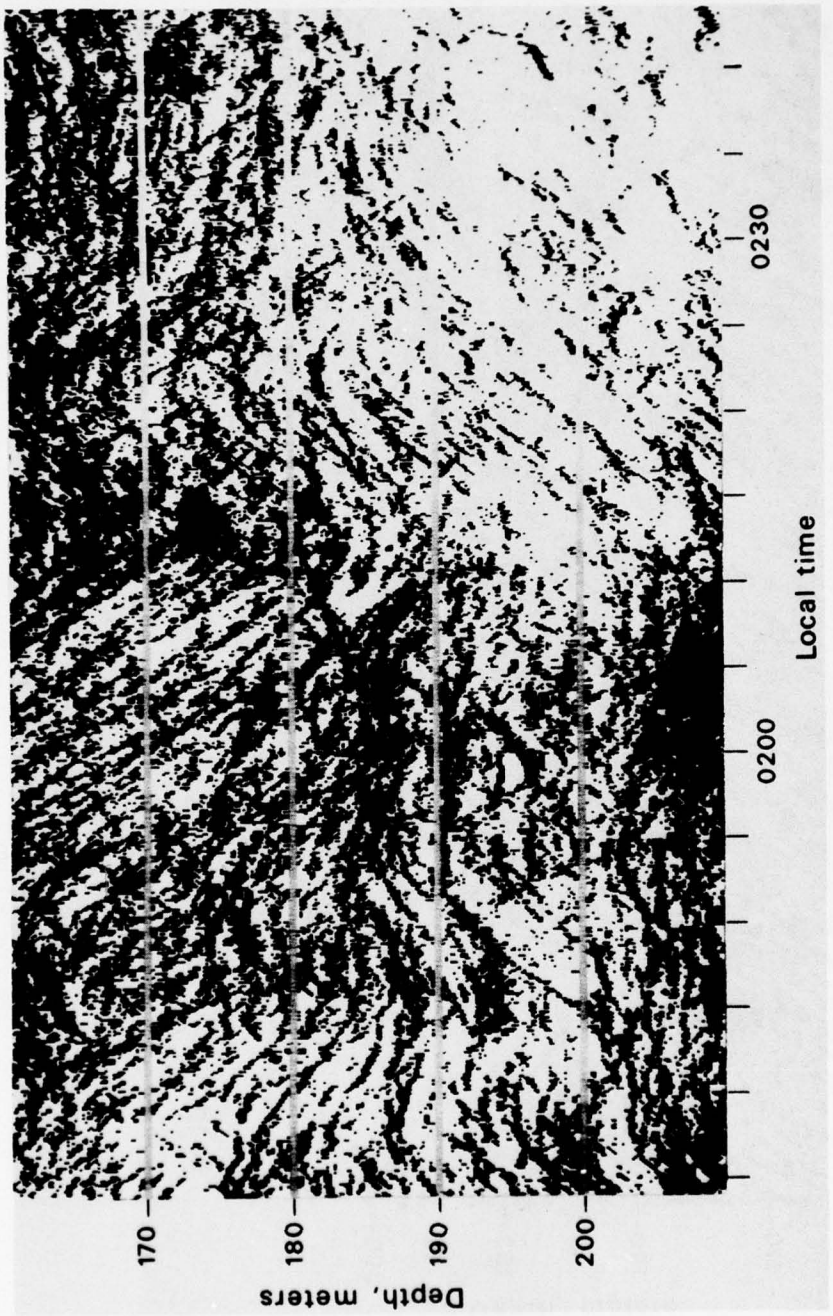

Figure 3b. Enlarged target strength record showing discrete scatterers and wave motion.

These and other expanded portions of the record were used to estimate target density. Within each 10 m depth increment and over a 1.1-hr period, the number of scatterers detected on ten spaced samples was counted by eye. Figure 3 represents the worst case of merged targets where estimates of numbers of targets were made. The other data record contained far fewer scatterers allowing a more precise counting. The expected number of scatterers per sample in a 10 m depth bin was then calculated as a mean of the ten countings. The insonified volume for this range increment was calculated from the beam directivity pattern and included the first sidelobe. Other sidelobes were determined to be insignificant because of the combination of the transmitted and received patterns. A set of 51 scatterer estimates was collected in this manner.

Next an echo-counting technique was employed to provide similar scatterer counts by totalling the target strengths calculated in identical 10 m depth bins for a single sample. The numbers of calculated target strengths were accumulated for 4000 consecutive samples. This total is then an indicator of scatterer density within the range bin over a 1.1-hr averaging period. It is assumed that the scatterers are distributed randomly within the range increment and homogeneously over time. We know that the scatterers are discretely identified for most of the data, so that multiple scattering was minimal. Again the scatterer concentrations in Figures 3a and 3b are atypical. Most of the expanded plots were similar to the region of Figure 3a bounded by 190-210 m in depth and in time by 0030-0050. Figure 4 is a straight-line fit between the scatterers counted by an observer and total numbers of target strengths calculated. Over two orders of magnitudes this fit is very good with discrepancies never greater than a factor of three. Based on this the remaining data were analyzed for scatterer count by using total calculated target strengths.

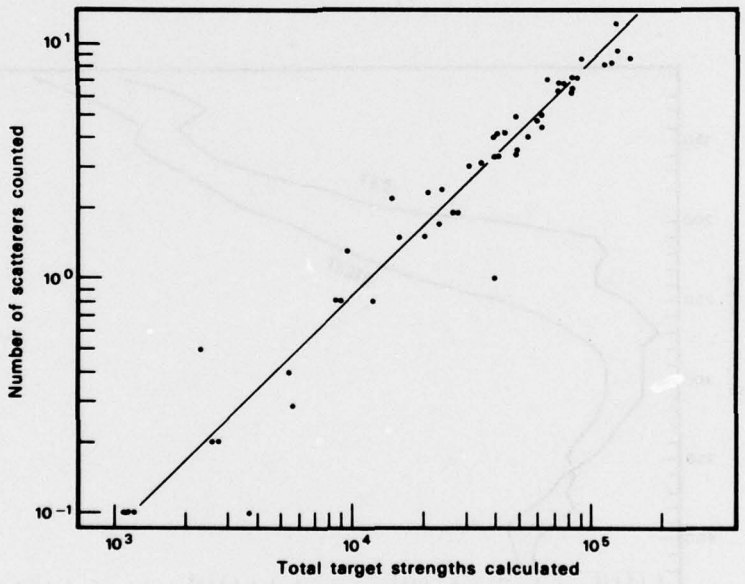

Figure 4. Comparison between estimated number of scatterers per sample in a 10 m range interval and total target strengths calculated within the same interval over a one hour period.

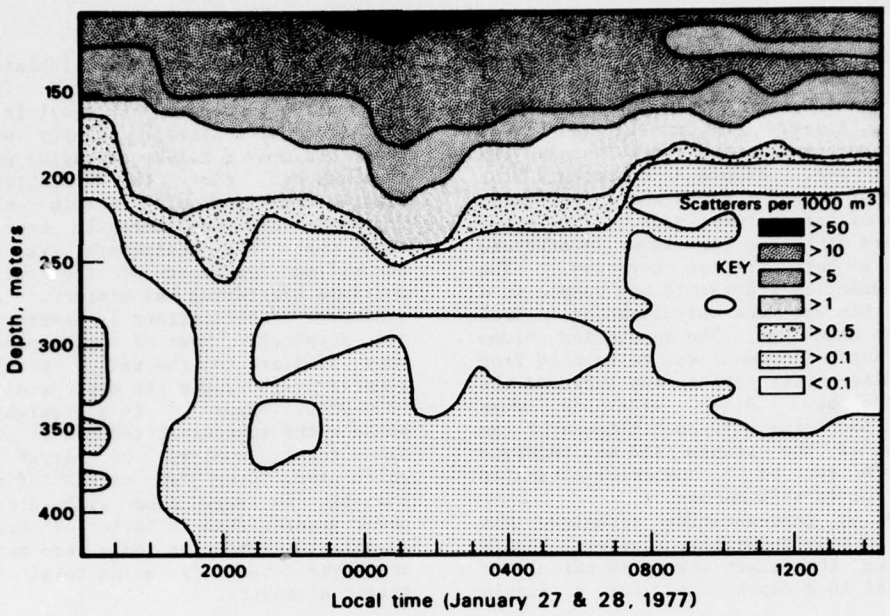

Figure 5. Acoustic scatterer density contour plot.

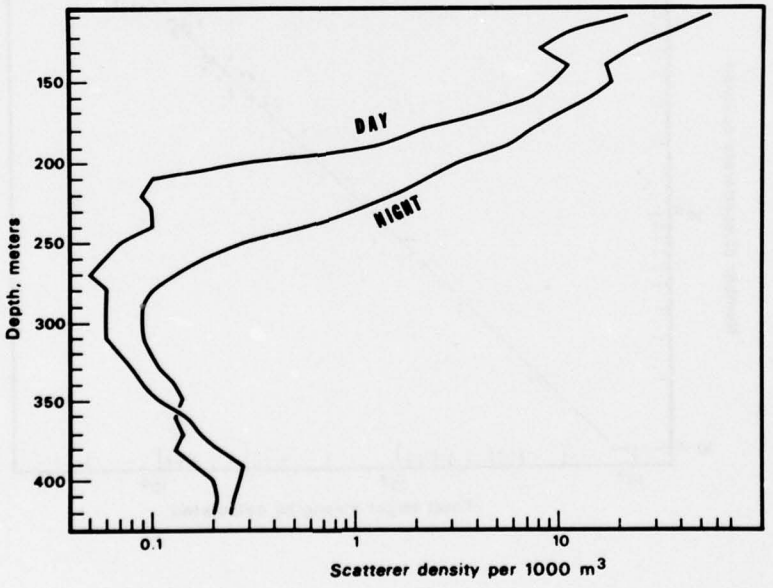

Figure 6. Day-night comparison of depth profiles of acoustic scatterer density.

A scatterer density contour plot for the January 1977 data is shown in Figure 5. The vertical migration of the Deep Scattering Layer (DSL) can be seen at both 2000 and 0700. The midnight migration appears as a large perturbation of the ambient scatterer densities. As a guideline for this information, we can use the data of Vent and Pickwell (1977), who obtained net haul and trawl data from the upper 400 m off of Baja California. Fish densities ranged from 2-20 fish per 1000 m^3. Densities of organisms that were not fish ranged from 10-1000 individuals per 1000 m^3, and included copepods, amphipods, euphausiids and squid, among others.

A day-night comparison of the scatter density vs. depth profiles is shown in Figure 6. Above 200 m the scatterer density is approximately twice as great during the night with respect to the day. This is reversed at 400 m where a resident population exists. However this decrease in density with depth is partially due to system limitations which precluded observation of weaker targets at the more distant ranges. If the scatterers were fish, it is estimated that the scatterer density estimates may be low by possibly an order of magnitude, based upon the trawl data of Vent and Pickwell.

Target strengths associated with these scatterers ranged from -38 to -73 dB with a data base of nearly 10^7 calculations, with a trend of target strength increasing with depth. For the scatterers in Figure 3, the target strengths ranged from -50 to -69 dB, with a median of -66 dB. No correction was made for the directivity pattern in these calculations. Since the volume swept by the first sidelobe is much greater than the main lobe, the majority of the targets were probably detected through the sidelobe. Thus most of the calculated target strengths should be around 6-7 dB stronger. If so they then correspond well with the reported peak target strengths of Squier, et al. (1976), which were determined by displaying the data from an analog tape onto a scope to observe the peak strength of an individual scatterer.

SCATTERER IDENTIFICATION

Biological samples were not taken during this observation time; therefore, the identity of the scatterers can only be inferred from their characteristics: (1) the scatterers are discrete individuals capable of vertical swim speeds of up to 8 cm/sec; (2) target strengths ranged from -38 to -73 dB; (3) scatterer densities ranged from 0.05 to 50 individuals per 1000 m^3; and (4) there was vertical migration of some, but not all, of the scatterers. These characteristics suggest that the scatterers could be swimbladder fish, squid and/or siphonophores, rather than zooplankters like euphausiids or copepods.

The target strength of fish has been studied by numerous researchers and has been reviewed by Love (1971). In this paper he presents his laboratory results for fish from 16 different families. The lengths of the fish ranged 1 cm to 1 m. Acoustic frequencies ranged from 8 to 1480 kHz. From these measurements he fitted his data to calculate maximum target strength to:

$$T_D = 19.4 \log L + 0.6 \log \lambda - 24.9, \text{ dorsal aspect} \quad (1)$$

$$T_D = 22.8 \log L - 2.8 \log \lambda - 22.9, \text{ side aspect} \quad (2)$$

where T is target strength in dB and L and λ are the fish length and acoustic wavelength in meters. Figure 7 is a plot of these relationships for a frequency of 87.5 kHz. Plots of (1) for 50 and 200 kHz are similar to those in Figure 7, but are displaced 0.2 dB higher and lower. From this we can see

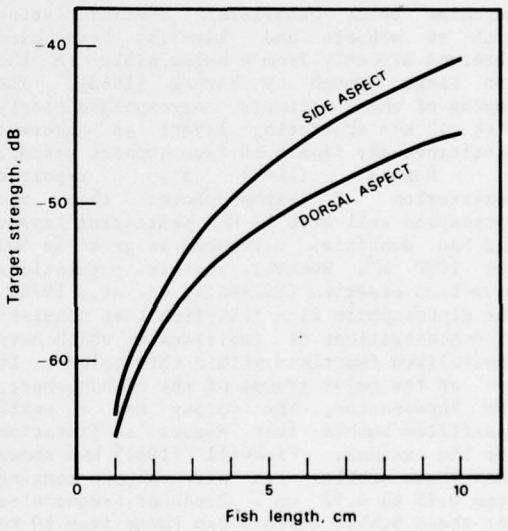

Figure 7. Plots of target strength vs. fish length for two aspects and for an acoustic frequency at 87.5 kHz, according to Love (1971).

that fish length is the dominant factor in determining acoustic strength and that the aspect is also more important than the acoustic wavelength, for frequencies much above swimbladder resonant frequencies. Other researchers have produced similar relationships, but the important point is that this range of target strengths agrees with the range of target strengths that were calculated. The fish lengths in Figure 7 are within the range typical of DSL fish. The vertical swim speeds of fish compare with the scatterer velocities that we have seen. Typical fish densities from trawl data are in the range of our calculated scatterer densities, except for those limited concentrations greater than 20 individuals per 1000 m^3. In summary the scatterer characteristics agree well with what we would expect for typical fish populations.

Another possible organism for the observed scatterers is the squid. Matsui, Teramoto and Kaneko (1972) made laboratory measurements of target strengths of 11 squid with mantle lengths of 11 to 12 cm. The maximum target strengths were about -45 dB at 50 kHz and -42 dB at 200 kHz. Although this was a very limited data set, it does show that the squid can be an important target. It is interesting that the target strengths, while slightly stronger, compare favorably with what we would expect for similarly-sized fish. Density of these animals is not well-known because of the difficulty in catching them; behavioral characteristics such as schools and layering have been observed directly from a submersible in the San Diego Trough by Barham (1963). The depths of these schools corresponded poorly with 12 kHz scattering layers as observed simultaneously from a surface support vessel.

Barham (1963) also reported observation of siphonophores that did correspond well with 12 kHz scattering layers and had densities estimated as great as 300 per 1000 m^3. However, sparser populations have been observed (Pickwell, et al., 1970). The siphonophore is a jellyfish that consists of concentrations of individuals which have specialized functions within this colony. In one of the major groups of the siphonophore, the Physonectae, the colony has a small gas-filled bubble that serves as flotation for the animal. Pickwell (1967) has shown that these bubbles can have volumes ranging from 0.25 to 4.92 mm^3. Resonant frequencies for these bubble volumes can range from 10 to 28 kHz at 100 m depth, and from 20 to 53 kHz at a depth of 400 m. Target strengths for these bubble volumes at 87.5 kHz should range from around -59 to -67 dB. The siphonophore can swim vertically, both upward and downward, and can sink from the surface in rough weather. It is capable of varying the bubble volume rapidly, adapting to sudden changes in pressure of half an atmosphere. Thus the animal would be capable of varying its bubble during migration and changing its acoustic characteristics dramatically. More quantitative measurements of animal density are difficult because the animal is most often destroyed by coming into contact with net hauls. Gas bubbles in preserved laboratory specimens have remained intact for a period of three weeks; in the water column these bubbles could then conceivably retain their acoustic strength after the death of the animal.

Smaller animals have been observed with high-frequency echo sounders, but not as individuals, and generally at shallower depths corresponding with the top of the thermocline. Barraclough, LeBrasseur and Kennedy (1969) tracked a shallow, 20 m thick layer of copepods with a 200 kHz echo sounder over most of a traverse of the North Pacific Ocean. The layer was usually at depths between 20 and 40 m and peak densities were on the order of 100 copepods per m^3. Friedl, Pickwell and Vent (1977) found good correlation between scattering layers and patches at 12 and 38 kHz in the upper 100 m and the distribution of pelagic crabs off southern Baja California. Cooney (1969) and Pieper (1977) correlated euphausiid distributions and scattering layers at around 100 kHz in Saandich Inlet in Puget Sound and the Santa Catalina Basin off southern California, respectively.

In all of these papers the scattering layers appear as dense concentrations of scatterers rather than as individuals, because of system resolution. It is also due to the weak target strengths of these animals. Cooney (1969) estimated target strengths at 102 kHz to be -90, -107, and -114 dB, for euphausiids, amphipods and copepods, respectively. These estimates were based upon typical animal volumes and measurements of animal compressibility reported by Beamish (1971). Greenlaw (1977) made direct measurements of target strength of preserved specimens of euphausiids and copepods in the laboratory. Around 200 kHz euphausiids and copepods were found to have strengths of -80 and -100 dB. Around 100 kHz the target strength of a euphausiid was measured at around -75 dB, while no value was given for copepods.

If we assume target strengths of -75 dB for euphausiids and -100 dB for copepods at 87.5 kHz, we can compare their strengths relative to fish. We will also assume that the backscattering from individual zooplankton will add with random phase. A typical DSL fish length of 35 mm (Vent, personal communication) should have a dorsal aspect target strength of around -55 dB.

Given these assumptions we calculate the following scattering strength comparison:

$$1 \text{ fish} = 10^2 \text{ euphausiids} = 2.9 \times 10^4 \text{ copepods} \quad (3)$$

We shall consider this as merely a guideline in comparing these animals. In addition we will have to consider the total volume insonified to match scattering strengths.

DENSITIES OF EUPHAUSIIDS AND COPEPODS

Ambient densities of euphausiids in the California Current System have been reported by Brinton (1967) as ranging from 20 to 100 per 1000 m^3. During daytime these animals are distributed in depth range of 150 to 200 m depending upon species. At night these animals migrate to the upper 100 m of the water column. Difficulties in capturing euphausiids in a standard net haul indicate that these estimates could be low by as much as a factor of ten. The euphausiids will swarm with patch densities ranging as high as 1-5 individuals per m^3 off Oregon (Greenlaw, 1977) which agrees with the values of 0.4-4.6 per m^3 found by Pieper (1977) in the Santa Catalina Basin.

Copepod densities off Baja California have been reported by Longhurst (1967). Peak densities were around 400 animals per m^3, which corresponds roughly with the value of 100 per m^3 found by Barraclough, et al. (1969). Longhurst found that depths of maximum densities varied between 100 and 300 m and that they did not migrate as part of the DSL. Depths of maximum densities varied from station to station. A secondary density maximum was found to occur between 60 and 90 m depth. There was a marked tendency for the copepods to layer in depth.

To finish our scattering strength comparison, we select a one-way range of 200 m, where the insonified volume of the 87.5 kHz system will be around 100 m^3, if the pulse duration is 1 msec and the first sidelobe of the directivity pattern is included. In this volume we may expect to find one fish, 5×10^2 euphausiids or 4×10^4 copepods, if peak plankton densities are assumed. From this we calculate that the scattering strength of the fish will be around 1 dB weaker than returns from the copepods and 6½ dB weaker than the euphausiids.

We have structured this exercise to provide the strongest case for the smaller animals. With ambient plankton densities, shorter pulse durations, and closer ranges, we can see that the dominant scatterer below the mixed layer will be the nekton. Plankters may be observed acoustically but probably as either swarms or as a limited number of thin scattering layers. Within the mixed layer, there appear to be sufficient plankton densities, both during night and day, so that they will be more dominant scatterers than individual fish but not fish shoals.

INCREASING TARGET STRENGTH WITH DEPTH

An increase in peak target strength with depth has been reported by Squier et al. (1976) as a repeatable trend for several observation periods within the same oceanic area off San Diego. Generally peak target strengths at 150 m were around -60 dB and increased to around -47 dB near 400 m. These were verified to be clean returns from individual scatterers. This correlates with results for the January 1977 data except for times of DSL migration. At an acoustic frequency of 87.5 kHz, changes in target strength of either siphonophores or fish because of bubble volume changes or pressure effects on bubbles are insufficient to explain this 13 dB increase. Instead this implies that the physical size of the targets increased with depth. If the scatterers were predominantly fish, this effect could be explained from Figure 7 as an increase in peak fish length from near 2 cm at 150 m to approximately 10 cm at 400 m.

A simple explanation of why the size of pelagic organisms should increase with depth is difficult, but has been reported as a general trend (Tseytlin, 1975). One observation made by several researchers (e.g., Kobayashi, 1973; Gibbs and Roper, 1970) is that within a given fish species, juveniles are caught at depths shallower than those of adult catches. Another observation of Kobayashi is that species within the mesopelagic fish genus, Cyclothone, tend to select different depth habitats. This has been corroborated by Tseytlin (1976), who reported species depths of both Cyclothone and Taaningicthys. The four reported species of Cyclothone increased in average size from 3 cm at 400 m to 7 cm at 800 m. Of the three species of Taaningicthys average length increased from 6½ cm around 500 m to 9½ cm at 900 m. Although these were preliminary results and were for fishes whose depth habitats are near or below the observation depths of the FLIP data, they do support the concept of increased fish length with depth. A third possibility is that the identity of the scatterers changes with depth. Around 150 m the scatterers could be predominantly siphonophores and smaller fish of approximate length, 2 cm, which should have target

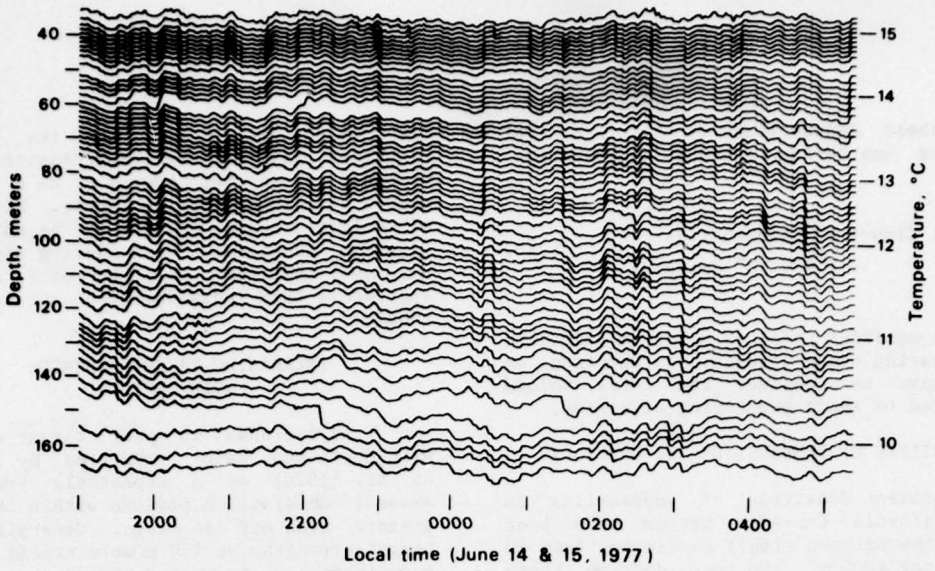

Figure 8. Isotherm depth fluctuations as a function of time. Isotherm contour increments are 0.1 C°.

strengths near -60 dB. Between 150 and 400 m, hatchetfish and lanternfish with lengths of 3 to 7 cm, typical in size and depth habitat, should have target strengths in the range of -50 to -59 dB. Around 400 m, larger fish and squid, with sizes near 10 cm, should have target strengths of -45 to -49 dB.

Documentation of these possibilities is insufficient to make a definitive statement. However, the depth increase in peak target strength is real and the suggestion that the size of the pelagic fauna increases with depth is a plausible explanation for this effect.

SOUND SCATTERERS AS INTERNAL WAVE TRACERS

We have shown that scatterers observed with the MPL 87.5 kHz echo sounder are probably nekton. We have also seen that because of the mobility of these organisms, they can at times have vertical swim speeds greater than internal wave vertical velocities. During times of vertical migration they may be poor indicators of water parcel motion. Most of the time this will not be true. The siphonophores are relatively slow-moving and generally inactive organisms at times other than during migratory periods (Barham, 1970). Barham also reports that many swimbladder fish like hatchetfish and lanternfish are not active swimmers during the day. Rather they go into a torpid state and may assume a motionless heads-up orientation. Based on his direct observations from a submersible, he noted that even at night in the upper 100 m of the water column, about 70% of the myctophids were active and swimming horizontally. Squid have also been observed motionless in a vertical orientation. From this we may find that these animals, while capable of vertical mobility, may still serve as tracers of water motion.

One indication of this has been made by Proni and Apel (1975) using a 20 kHz echo sounder mounted upon a moving surface ship. Although these authors suggest the possibility that their returns may be due to density microstructure, the acoustic records in the paper show little data in the upper 100 m prior to the rise of the DSL. After the scattering layer has risen, however, they found good correlation between scattering layer depths and temperature gradient structure and between scattering layer fluctuations and observed temperature variations as sensed with a thermistor that was towed at a depth of 31 m. It is more likely that their scattering is due to biological reverberation, but the internal wave information does apply to our present topic.

A more definitive comparison was accomplished with isotherm fluctuation data taken on 14-15 June 1977 and an 87.5 kHz echo sounder record. Water temperature and conductivity were profiled from R/P FLIP every 125 sec to a depth of 180 m. Details of the yoyo profiler are given in Pinkel (1975). Figure 8 is an isotherm-depth vs. time plot for this observation period. High frequency, 3-7 cph, internal waves can be

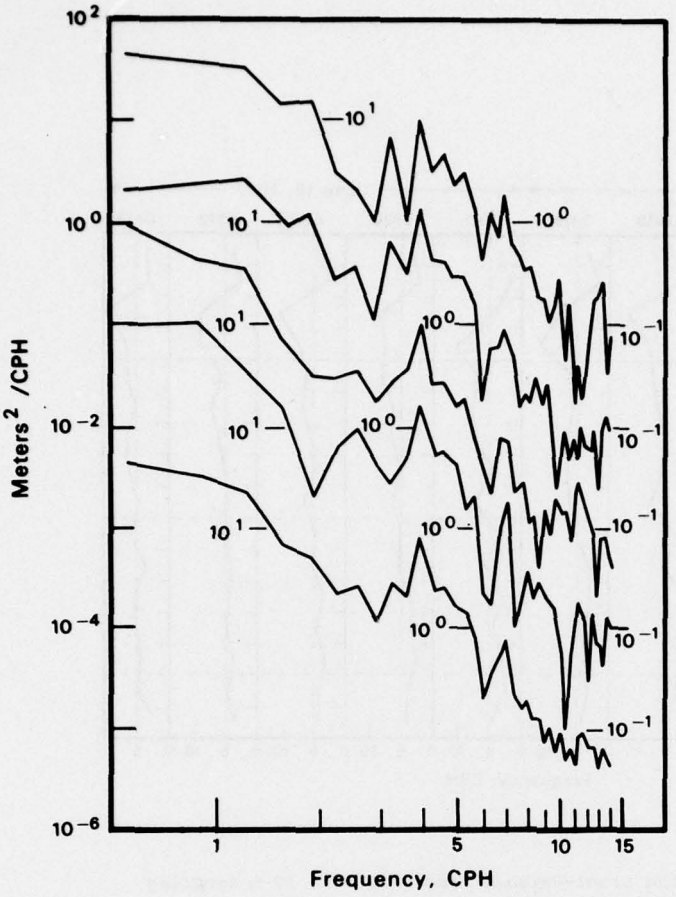

Figure 9. Isotherm vertical displacement spectra from record length of 8.9 hr and a Nyquist frequency of 14.5 cph.

seen throughout the record. These waves generally have vertical coherence over the entire sampled depth range and are probably first mode waves. Pinkel has shown that this is not surprising, since most of the high frequency energy observed by him was dominated by the first mode. The spacing of the isotherm contours, which are in increments of 0.1 C^o, give a good indication of the temperature gradient. Around 150 m there is a relatively isothermal region which is 10-15 m thick. The 10 m drop of the 10.1^o isotherm around 2220 indicates that the apparent vertical motion was not real but was actually due to the fact that temperature is a poor water motion tracer in isothermal water. However, for most of the record, the isotherms appear sufficient for our purpose. The top of the record corresponded approximately with the top of the thermocline. For this work we will assume that isotherm depth fluctuations will infer changes in the rms potential energy

$$E = \tfrac{1}{2}\rho\, N^2(z) \quad \langle \eta^2 \rangle \qquad (4)$$

where ρ is density, η is the displacement of an isopycnal about its mean position, and $N(z)$ is the Brunt-Vaisala frequency, given by

$$N(z) = (g/\rho\ (\partial\rho/\partial z - \rho g/c^2)\ )^{\frac{1}{2}} \qquad (5)$$

where c is the speed of sound in water and g is the acceleration due to gravity.

The frequency spectrum of the isotherm vertical displacements is related to the spectral density function and is thus an indicator of internal wave potential energy with frequency. Isotherms at initial depths of 100, 120, 140 and 160 m were tracked over an 8.9 hr period with a Nyquist frequency of

Isotherm displacements were centered about a zero mean and a triangular data window was applied to them. These 256-point data records were then fast Fourier transformed. The resulting four spectra are plotted in Figure 9 and have been offset successively by 10 dB increments. Actual values are indicated relative to each spectrum. The fifth spectrum is a composite

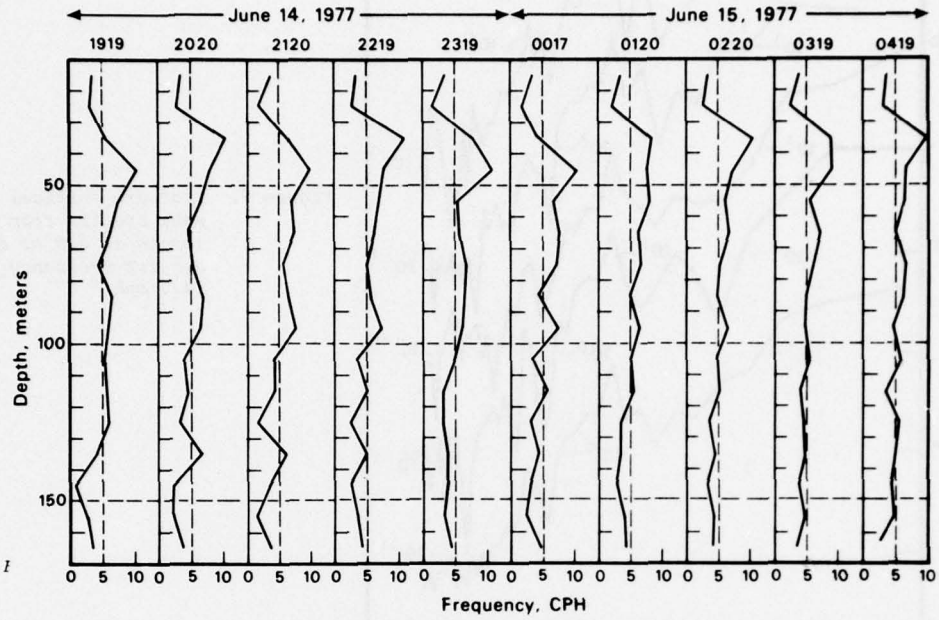

Figure 10. Depth profiles of the Brunt-Vaisala frequency on a 10 m sampling interval from yoyo profiler information.

of the four data records with approximately 32 degrees of freedom. The 90% confidence limit for the values of this spectrum is around $\pm 2\frac{1}{2}$ dB. Generally the spectra fall off to around 3 cph. Between 3 and 5 cph there is an energy plateau, followed by a roll-off of 7 dB. A real energy spike occurs around 7 cph, with another drop-off to the noise level at 10^{-1} m^2/cph.

Using both the temperature and conductivity data from the profiler, water density was calculated and profiles of the Brunt-Vaisala frequency (BVF) with depth were determined. Sound speed was not measured but was estimated from the data according to the equation of Wilson (1960). At first the BVF was calculated on two-meter intervals and showed several regions of static instability. Some of these are due to sensor limitations for this purpose. However, Lee (personal communication) found similar unstable regions as determined with profiles from XSTD samplings, indicating that this was a dynamic region of the thermocline. This is an area where the cold less-saline water of the California Current is mixing with warmer more-saline water coming from the south. Because of this, this region is rich in microstructure activity as these water masses interleave and mix. The BVF was recalculated on 10 m intervals which produced no static instabilities. Figure 10 is a series of these profiles from data taken throughout the observation period. It can be seen that the BVF varied in the depths 70-170 m between 3 and 7 cph, which is what we would have expected based upon the spectral information alone.

ACOUSTIC INFORMATION

Figures 11a through 11f show the entire acoustic record for this observation period. The pulse duration was 0.1 msec. A surface reflection from the backlobe of the array can be seen at 170 m. The receiver was saturated for the first 12 m of the record. The rise of the DSL can be seen in Figure 11a as at least two populations. The first is from a group of scatterers at around 230 m which began ascending around 2000. The second group began around 2020 and ascended at a greater rate. Some of the scatterers went above the start of the acoustic record. Prior to the rise of the scattering layers, a resident daytime population can be seen with concentrations at 110 and 120 m. Wave activity with total amplitudes as great as 9 m and with periods 10-12 min can be noted.

Figure 11b shows the nighttime conditions with little wave activity. Numerous scatterers show "tent-shaped" patterns often associated with feeding fish.

Figure 11c shows the diffusion of the scattering layers at 110 and 120 m, while there is a formation of a new scattering layer at 140 m.

Figure 11d is an active portion of the record with marked wave activity that appears to be in phase from 100 to 150 m. The 120 and 140 m scattering layers are still recognizable. Also around 0050 and at 115 m, we can see the formation of a new scattering layer that is qualitatively different from the others. This layer is quite dense and does not appear to be composed of scatterers that can be recognized as discrete. This scattering is probably due to zooplankton that may be associated with a wedge of water with different physical characteristics. Note that there are numerous scatterers that are migrating downward as individuals rather than as a layer.

Figure 11e is similar to the previous figure except that the dense scattering layer initially at 115 m has broadened to an approximate thickness of 15 m. The downward migration of scatterers is more pronounced.

Figure 11f, the end of the record, continues to show the dense scattering layer and also shows diffusion of the layer at 140 m. Downward migrating scatterers are beginning to concentrate around 230 m. A large concentration of scatterers is also forming around 100 m, obscuring information in the first 30 m of the record.

COMPARISON OF ACOUSTICAL DATA WITH ISOTHERM DEPTH FLUCTUATIONS

Figures 12a through 12f are a direct comparison between the wave activity seen in the acoustic record and the depth fluctuations of selected isotherms. Temperature data were available to a depth of 180 m, so that only that portion of the acoustic record is displayed. The isotherm contours are in increments of 0.25 C^{o}. The isotherms were not plotted on top of the acoustic record so that an observer would not be biased.

Figure 12a shows that the agreement between wave activities as sensed in the two manners is excellent in terms of both amplitude and phase. This correlation becomes more difficult as the DSL rises through our depths of interest. This is apparent for the 10^{o} isotherm at 2020. Here an oscillation of total amplitude 3 m can not be readily seen in the acoustic information. The scattering layer at 120 m is bounded top and bottom by the 10.25^{o} and 10.50^{o} isotherms. These isotherms diverge over the period of this figure and the scattering layer thickens accordingly. The 110 m layer has a lower bound of around 11^{o}.

Figure 12b is a period after the rise of the DSL and is a relatively quiet period in terms of wave activity. However, the oscillation between 2140 and 2150, with total amplitude of 3 m, is still recognizable. Although the temperature gradient in this depth band, as indicated by the spacing of the isotherms, does not vary greatly over this portion of the record, the scattering layer at 110 m disappears and the layer at 120 m diffuses. By 2200 it nearly ceases to be a layer.

Figure 12c shows the formation of a new scattering layer at around 140 m that appears tagged to the 10.25^{o} isotherm. At the start of the record this isotherm is at a depth of 130 m and descends to a depth of 143 m by 2310. This motion is accurately depicted in the acoustic record. At 2330 a 3 m oscillation of the 10.5^{o} contour is easily seen in the acoustic data, but the oscillation of the 9.75^{o} isotherm is less apparent. This may be due to a decreased scatterer density so that there are fewer water motion tracers that can be observed. This is also true for the 9.75^{o} isotherm near midnight.

Figure 12d shows that there were gaps in the profiler data so that the isotherm information is discontinuous. Depth fluctuations occur between 0010 and 0050 and are accurately reflected in the acoustic record. In addition to the scattering layers at 120 and 140 m, a new layer appears at 115 m around 0100. The start of this layer corresponds with the appearance of the 12^{o} isotherm in the data. The bottom of the scattering layer appears tagged to the 10.75^{o} contour. The downward migration of individual scatterers around 0100 makes the isotherm depth fluctuations more difficult to observe.

Figure 12e shows an active time with six oscillations of approximately 12 min period. Total amplitude is about 6 m. The dense scattering layer has broadened to a thickness of 15 m and has an upper bound given by the 11.2° isotherm. Correlation is again excellent. The large downward migration of individual scatterers around 0240 hinders but does not obscure the isotherm fluctuations.

Figure 12f shows the end of the record and has one obvious oscillation at 0355. The 140 m scattering layer has now diffused, or migrated, and the layer at 120 m has now been obscured by the very dense scattering layer of plankters. Again note that the 0355 oscillation of the 9.75° isotherm has a total amplitude of 3-4 m that is difficult to note in the acoustic record.

The conclusion that can be drawn from this comparison is that the acoustic record is an accurate indicator of internal wave motion for wave total amplitudes at least as small as 3 m. Smaller amplitude waves might be observed with a more-sophisticated data processing scheme. Just as importantly, the ability to observe oscillations degrades as the scatterer density decreases.

CONCLUSIONS AND RECOMMENDATIONS

1. The reverberation that is observed with the 87.5 kHz echo sounder is due primarily to backscattering from discrete individuals. These scatterers have densities ranging from 0.05 to 50 individuals/1000 m^3 in the 300 m of the water column immediately below FLIP.

2. Based upon the scatterer densities and their target strengths, these individuals are probably fish, and also possibly squid and siphonophores. Zooplankton have insufficient target strengths to be observed as individuals. While plankters can be observed if they have sufficient densities, they will generally occur as patches or as a limited number of dense scattering layers.

3. Because the dominant scatterers are nekton, they are capable of vertical mobility and some of them will participate in the diurnal migrations of the Deep Scattering Layer. Additional migrations may be triggered by environmental factors such as passing rain squalls or the onset of rough weather. During daytime these scatterers should be generally inactive and may serve as tracers of internal waves. At night these scatterers will be more active and should be less reliable tracers.

4. Peak target strengths were found to increase with depth from around -60 dB at 150 m to near -47 dB near 400 m. It is suggested that this effect may be explained as an increase in the physical size of the scatterers with depth.

5. A visual comparison between scattering layer motions and isotherm depth fluctuations showed excellent correlation for total wave amplitudes as small as 3 m. Smaller wave amplitudes might be observed with better processing techniques. The ability to make this comparison is dependent upon the scatterer density.

The fact that scattering layer motions correspond with small depth fluctuations of isotherms is quite heartening. Observations of smaller depth fluctuations might be possible with a data processing scheme and with improvements in the system performance. Increasing the pulse duration to greater than 1 msec will not help, since the half-ping length of this pulse is around 0.75 m. However, techniques which will increase the number of scatterers detected within a 1 msec pulse should increase the sensitivity of the internal wave observations. Fish trawl data suggest that our scatterer density should not fall off as rapidly as it does; rather, the increase of minimum target strength with depth suggests that system limitations are precluding observation of but the large scatterers that have been insonified.

System performance could be improved in several ways. First, one could use a slightly wider beamwidth. This will increase the probability of detecting a scatterer at a given range and should provide a longer look time at an individual water motion tracer. We have seen that the first sidelobe of the 87.5 kHz echo sounder was important in obtaining these data, so that we had an effective full beamwidth of around 4°. In a practical application this increased beamwidth must be weighed against the maximum insonified volume that would be acceptable. This in turn depends upon the most likely signal depths and the spatial distribution of the signal. Second, one may increase the source level and/or the initial gain through the receiver in order to improve the signal-to-noise ratio of the return. The disadvantage of this is that the receiver will be overloaded for a longer range than the 12 m in the present system. Third, one might implement an improved time-varying-gain. With the present receiver noise levels, the system is limited to depths of about 500 m. Lastly, one may consider using a lower acoustic frequency. The target strengths of these scatterers will probably be little-affected by working at 50 kHz, for example. However, when one considers the attentuation coefficients at frequencies of

50, 87.5 and 200 kHz for round-trip ranges of 1 km, the transmission loss due to attentuation could be decreased substantially by working at a lower frequency.

Of these recommendations we intend to implement a different time-varying-gain as the most feasible improvement to the present system. Although "ground truth" data from the yoyo profiler will not be available in the coming year's work, we intend to document if increased scatterer densities can be observed with this improvement and if there is a day-night difference in the internal wave observation capability.

* *

Acknowledgements. Discussions in both background information and manuscript preparation were held with F. H. Fisher and G. B. Morris of the Marine Physical Laboratory and with R. J. Vent, W. A. Friedl, I. E. Davies, O. S. Lee and C. F. Ramstedt of the Naval Ocean Systems Center. R. Pinkel and L. S. Tomooka of MPL provided the edited data from the yoyo profiler. Their help is gratefully acknowledged. This work was sponsored by the Advanced Research Projects Agency, ARPA Order Number 2127 and Program Code Number 7D40 and by the Office of Naval Research, Code 222, under Contract No. N00014-75-C-0549.

* *

REFERENCES

Barham, E. G. Siphonophores and the Deep Scattering Layer, Science, 140, pp. 826-828 (1963).

Barham, E. G. Deep-sea fishes: Lethargy and vertical orientation. From: Proceedings an international symposium on biological sound scattering in the ocean, Farquhar, G. B. (Ed.) (1970).

Barraclough, W. E., R. J. Lebrasseur and O. D. Kennedy. Shallow scattering layer in the subarctic Pacific Ocean: Detection by high-frequency echo sounder, Science, 166, pp. 611-612 (1969).

Brinton, E. Vertical migration and avoidance capability of euphausiids in the California Current, Limno. and Oceanogr., 12, pp. 451-483 (1967).

Cooney, R. T. Zooplankton and micronekton associated with a diffusive sound-scattering. Ph.D. dissertation, University of Washington (1969).

Fisher, F. H. and E. D. Squier. Observation of acoustic layering and internal waves with a narrow-beam 87.5 kHz echo sounder, J. Acoust. Soc. Am., 58(6), pp. 1315-1317 (1975).

Fisher, F. H. and V. P. Simmons, Sound absorption in seawater, J. Acoust. Soc. Am., 62(3), pp. 558-564 (1977).

Friedl, W. A., G. V. Pickwell and R. J. Vent. The Minox Program: An example of a multidisciplinary oceanic investigation. From: Oceanic Sound Scattering Prediction, Andersen, N. R. and B. J. Zahuranec, (Eds.) Plenum Press, New York , pp. 591-618 (1977).

Greenlaw, C. F. Backscattering spectra of preserved zooplankton, J. Acoust. Soc. Am., 62(1), pp. 44-52 (1977).

Longhurst, A. R. Vertical distribution of zooplankton in relation to the eastern Pacific oxygen minimum, Deep-Sea Research, 14, pp. 51-63 (1967).

Love, R. H. Measurements of fish target strength: A review, Fishery Bull., 69(4), pp. 703-715 (1971).

Matsui, T., Y. Teramoto and Y. Kaneko. Target strength of squid. Japanese Echo Sounding Research on Squid. FIRM/C142. Food and Agriculture Organization of the United Nations, Rome (1972).

Pickwell, G. V. Gas and bubble production by siphonophores. Naval Undersea Warfare Center, TP-8, 98 pp. (1967).

Pickwell, G. V., R. J. Vent, E. G. Barham, W. E. Batzler and I. E. Davies. Biological acoustic scattering off Southern California, Baja California, and Guadalupe Island. From: Proceedings of an international symposium on biological sound scattering in the ocean, Farquhar, G. B. (Ed.) pp. 490-507 (1970).

Pieper, R. E. Some comparisons between oceanographic measurements and high-frequency scattering (100 kHz) of underwater sound. From: Oceanic Sound Scattering Prediction, Andersen, N. R. and B. J. Zahuranec (Eds.) Plenum Press, New York (1977).

Pinkel, R. Upper ocean internal wave observations from FLIP, J. Geophys. Res., 80(27), pp. 3892-3910 (1975).

Proni, J. R. and J. R. Apel. On the use of high-frequency acoustics for the study of internal waves and microstructure, J. Geophys. Res., 80(9), pp. 1147- 151 (1975).

Squier, E. D., R. B. Williams, S. P. Burke and F. H. Fisher. High resolution, narrow beam echo sounder. Scripps Institution of Oceanography, SIO Reference 76-8, 15 pp. (1976).

Tseytlin, B. V. Gigantism in deep-water plankton-consuming organisms. Oceanology, 15(3), pp. 499-503 (1975).

Tseytlin, B. V. Relation of vertical distribution to length in pelagic plankton-feeders, Oceanology, 16(1), pp. 77-78 (1976).

Vent, R. J. and G. V. Pickwell. Acoustic volume scattering measurements with related biological and chemical observations in the northeastern tropical Pacific. From: Oceanic Sound Scattering Prediction, Andersen, N. R. and B. J. Zahuranec (Eds.) Plenum Press, New York, pp. 697-716 (1977).

Wilson, W. D. Speed of sound in sea water as a function of temperature, pressure, and salinity, J. Acoust. Soc. Am., 32, pp. 641-644 (1960).

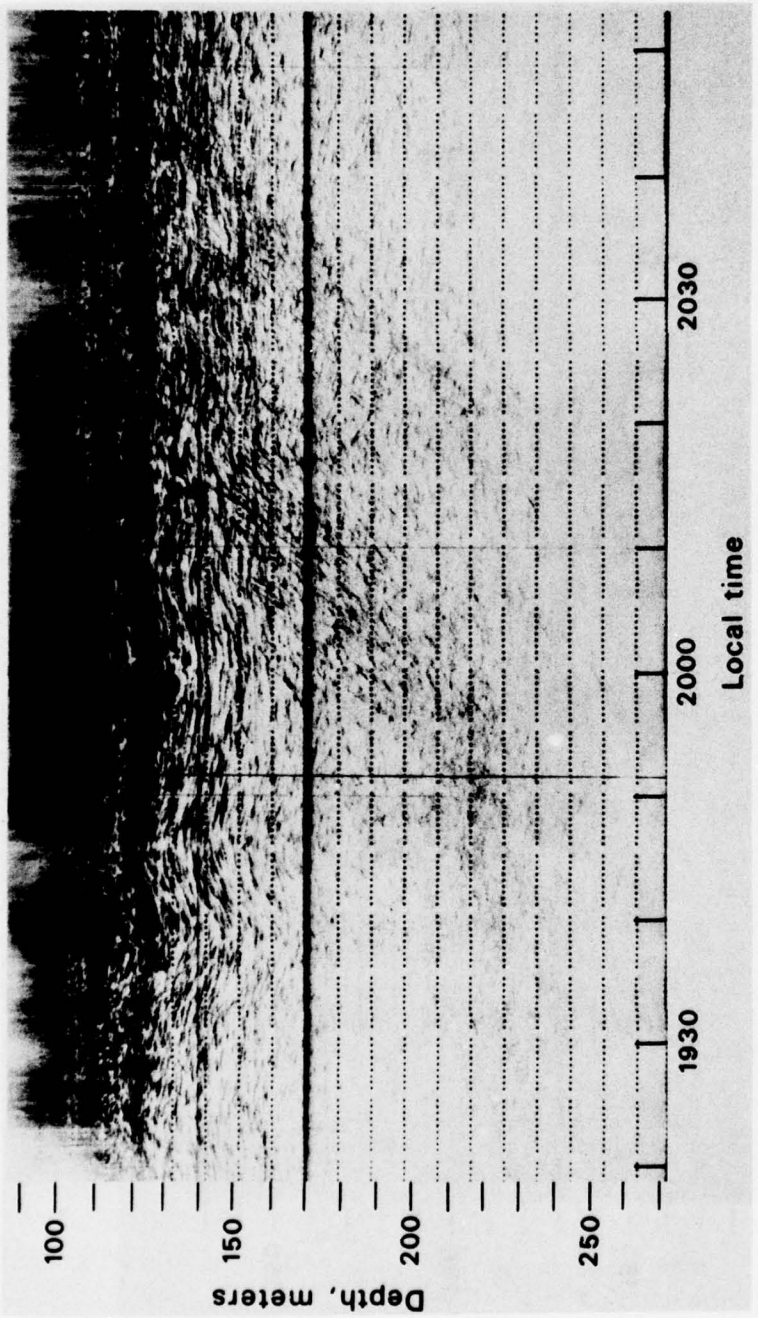

Figure 11a

Figures 11a - 11f. Analog recording of 87.5 kHz echo sounder from June 1977. Pulse duration was 0.1 msec.

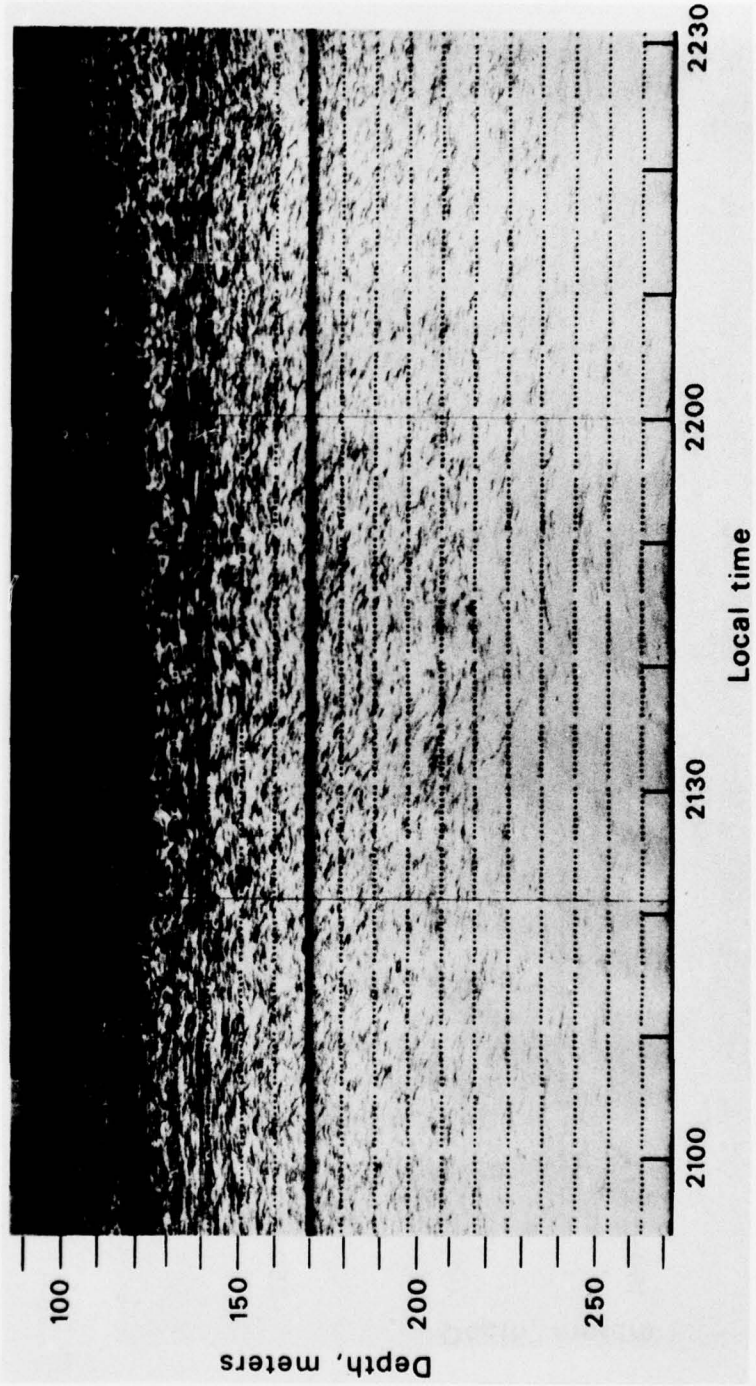

Figure 11b

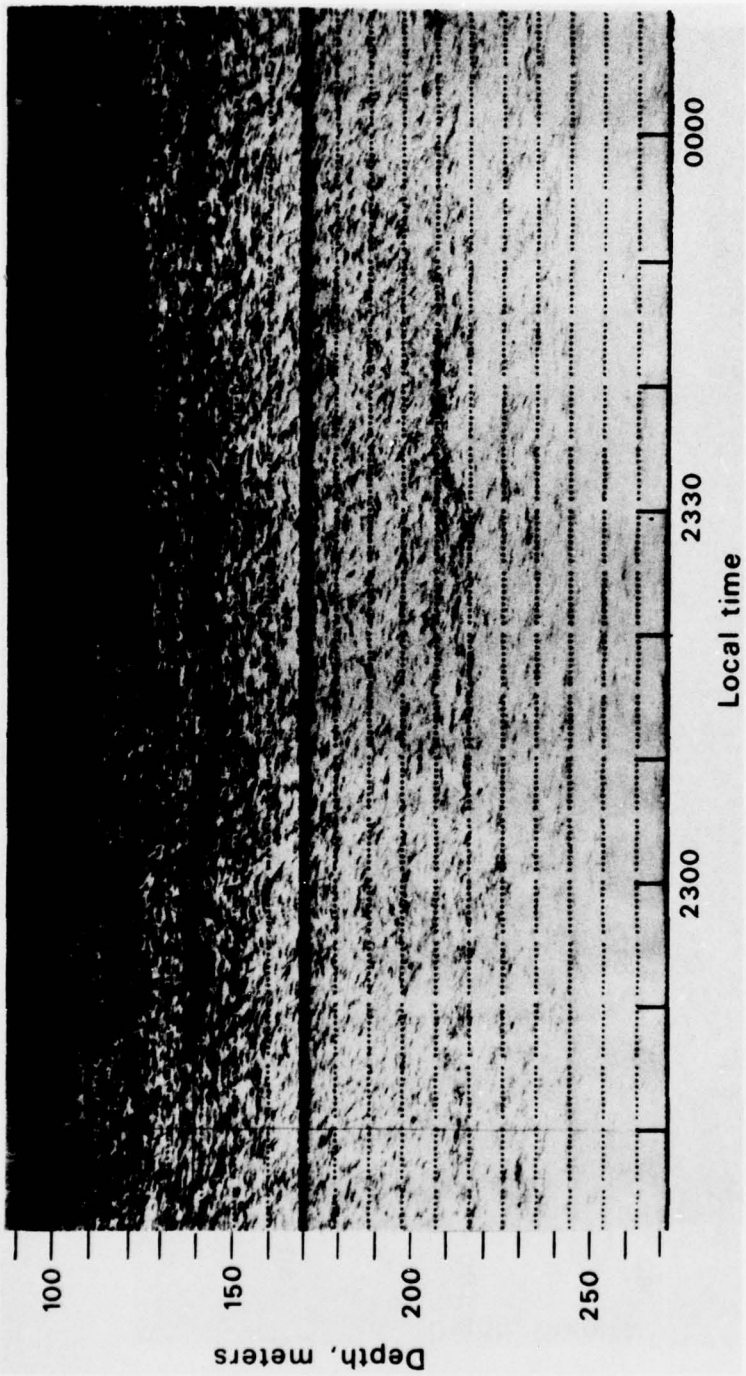

Figure 11c

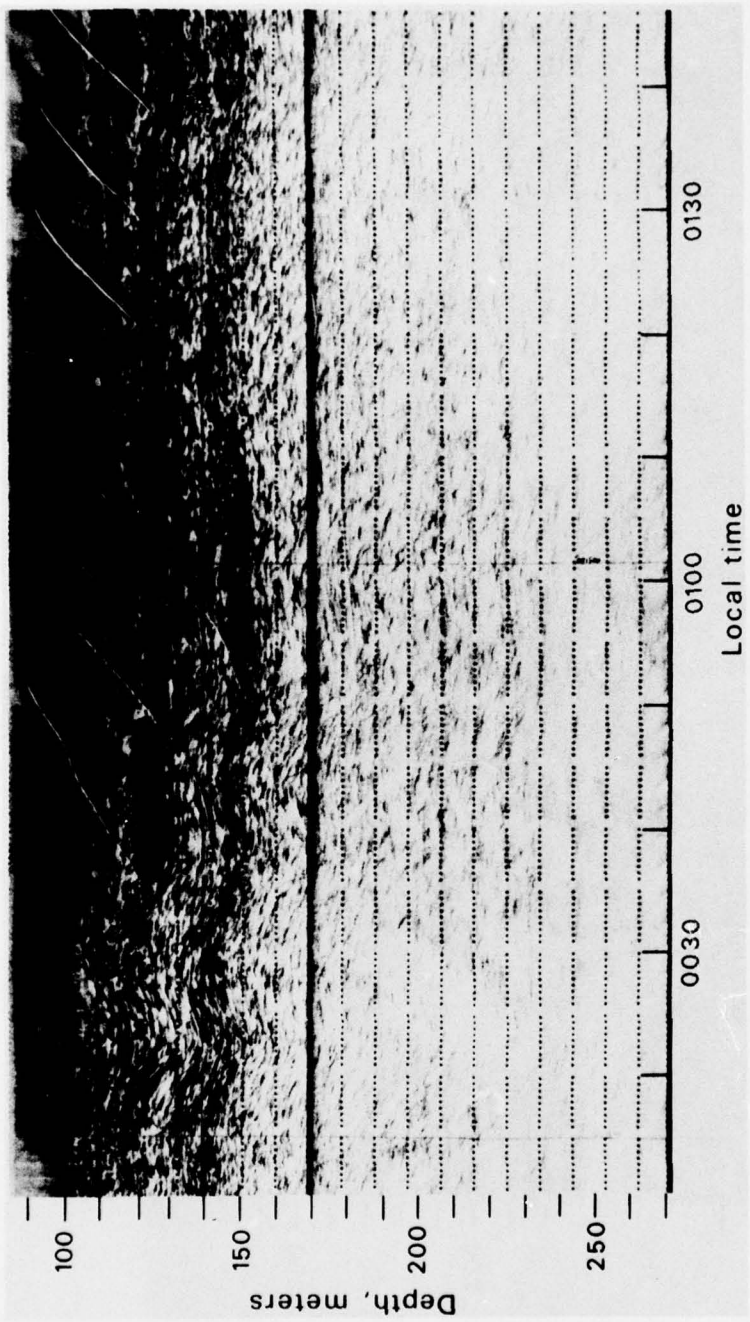

Figure 11d

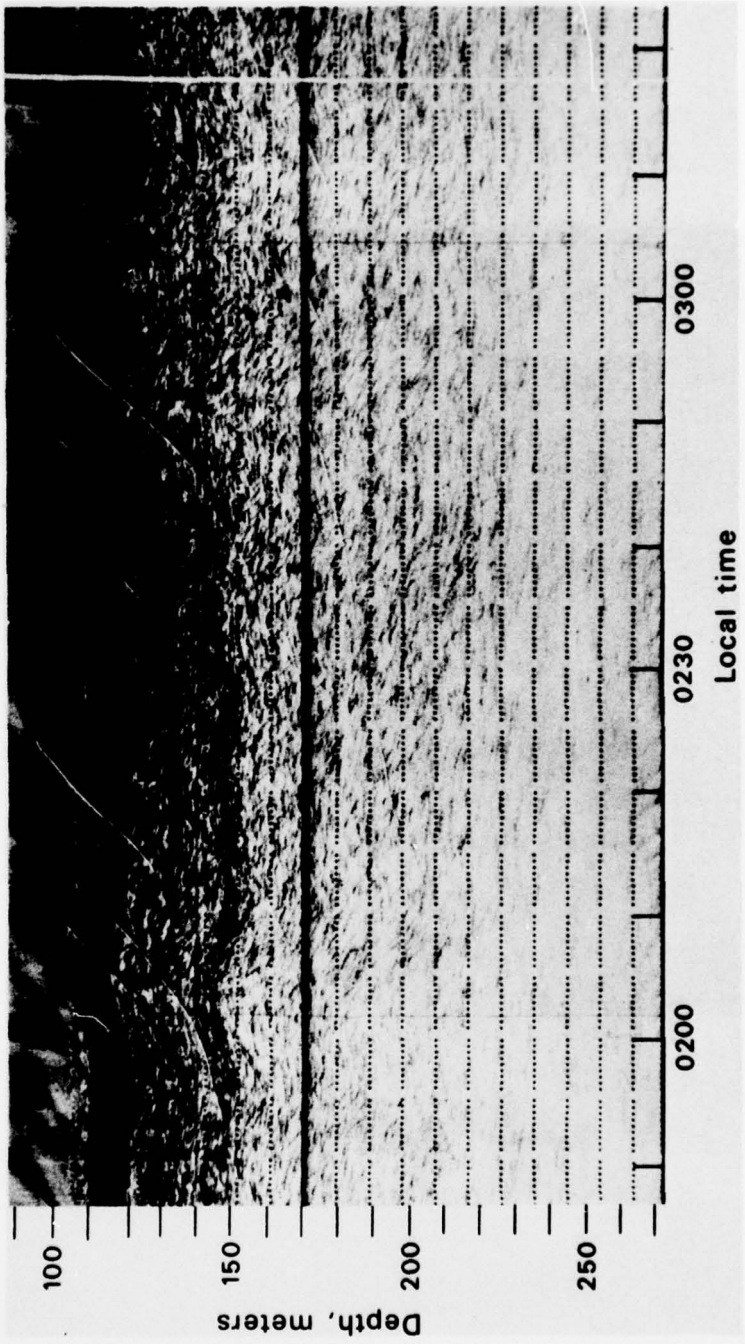

Figure 11e

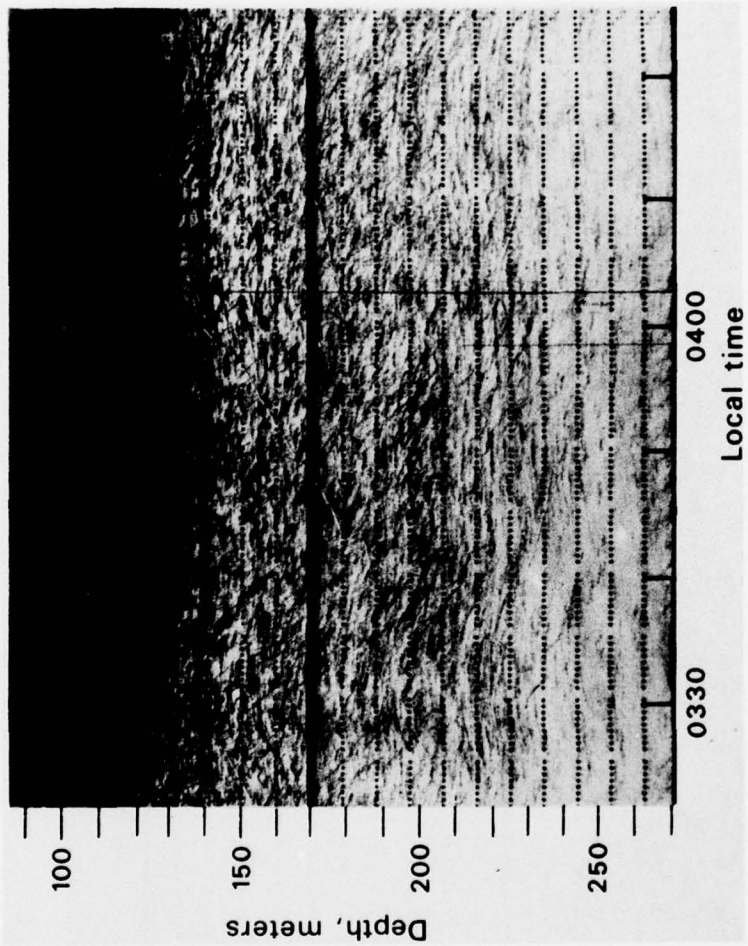

Figure 11f

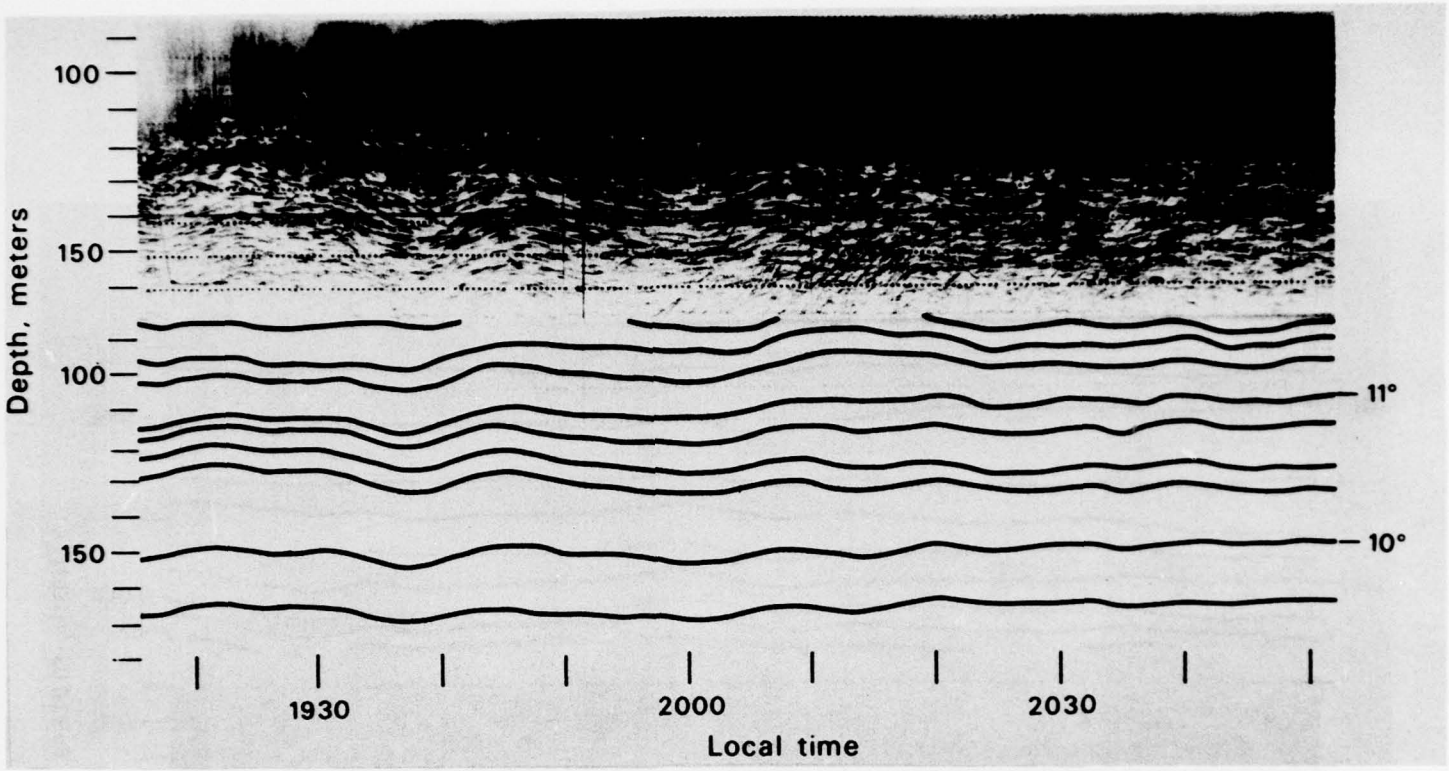

Figure 12a

Figures 12a - 12f. Dual plot of concurrent data from June 1977. Upper portion is analog recording of 87.5 kHz echo sounder data. Lower portion shows isotherm depth fluctuations. Contour increment is 0.25 C°.

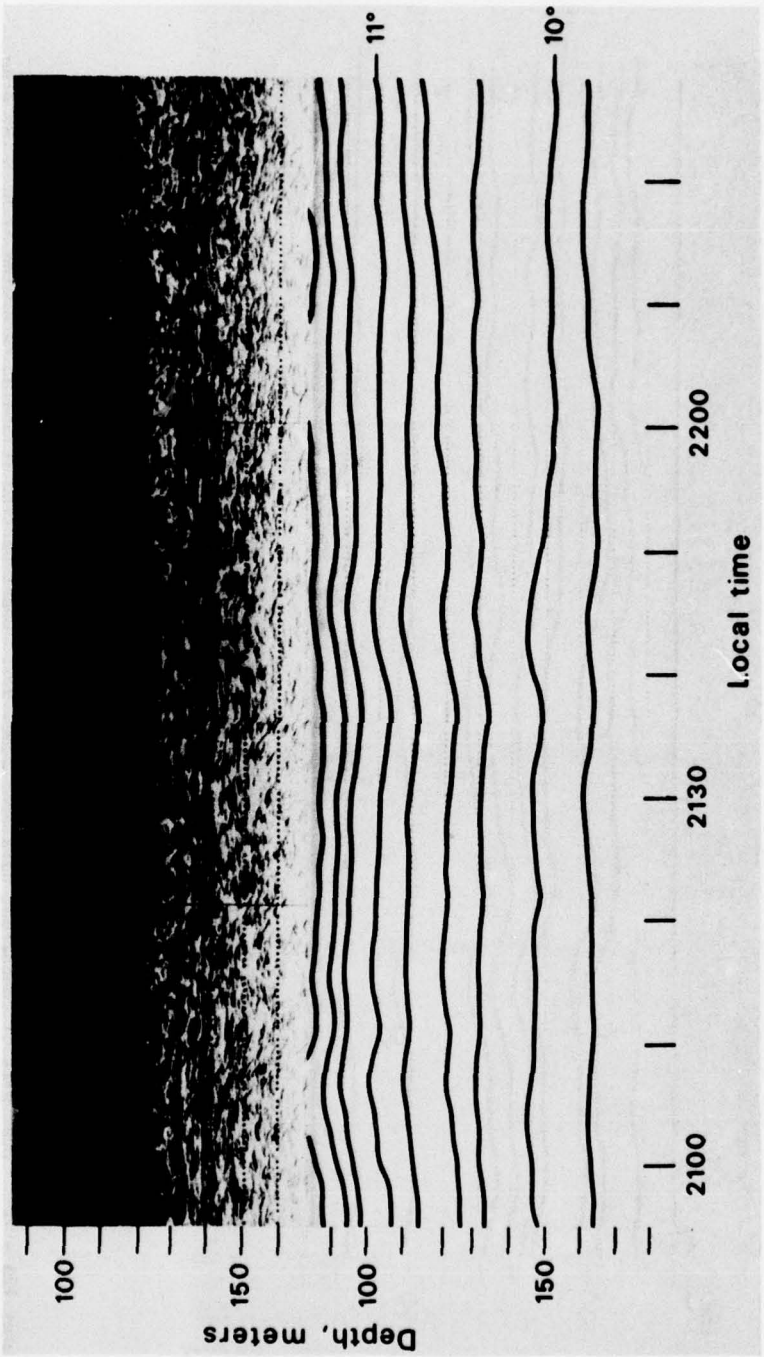

Figure 12b

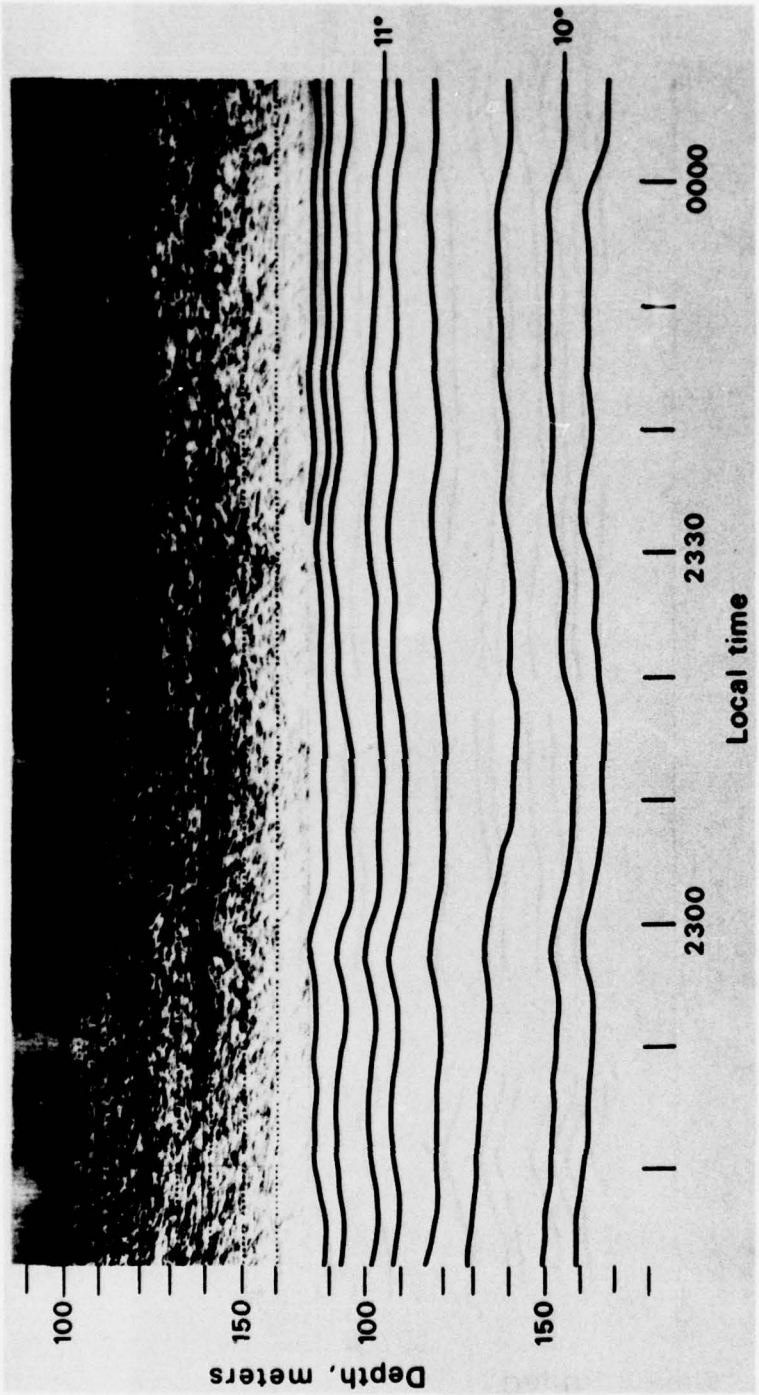

Figure 12c

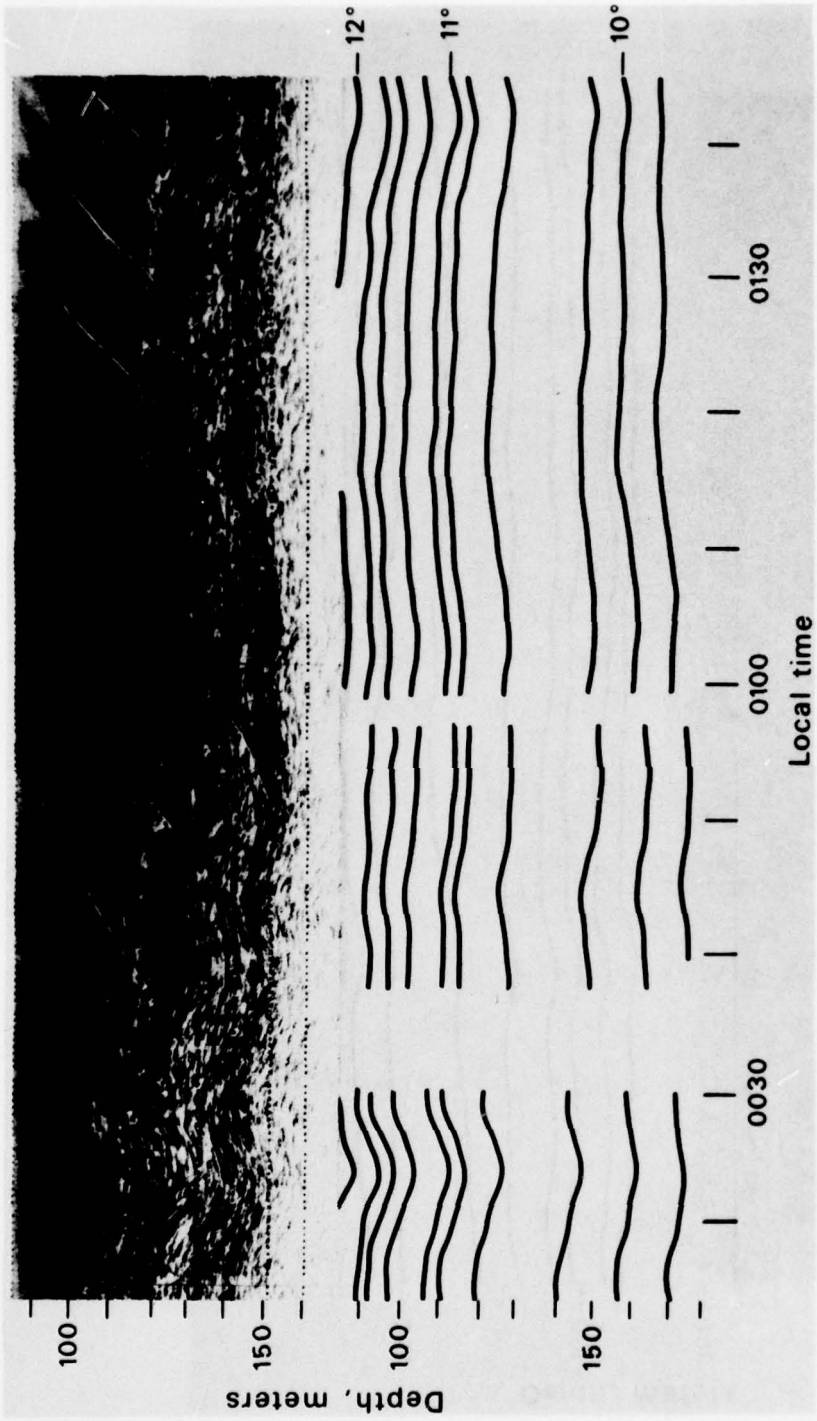
12°
11°
10°
100
150
100
150
Depth, meters
0030
0100
0130
Local time

Figure 12d

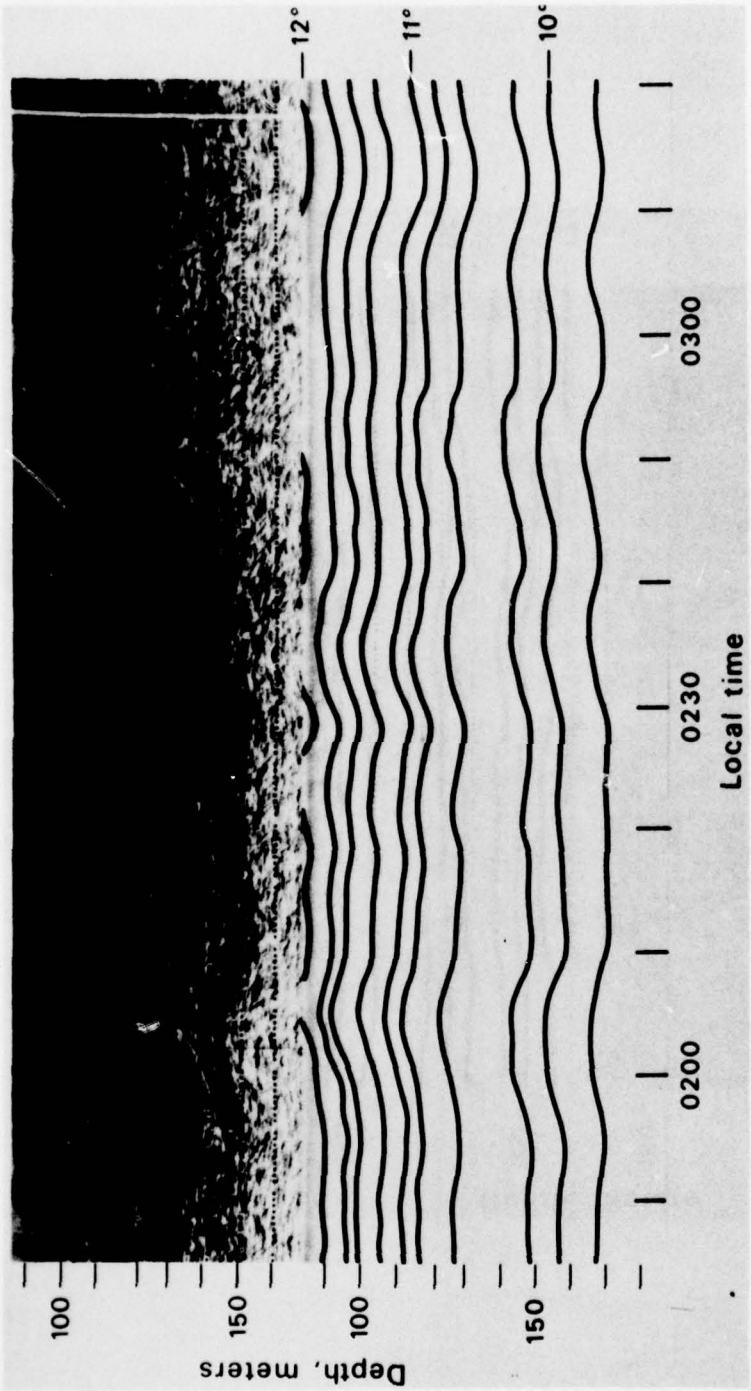
12°
11°
10°
0200
0230
0300
Local time
100
150
100
150
Depth, meters

Figure 12e

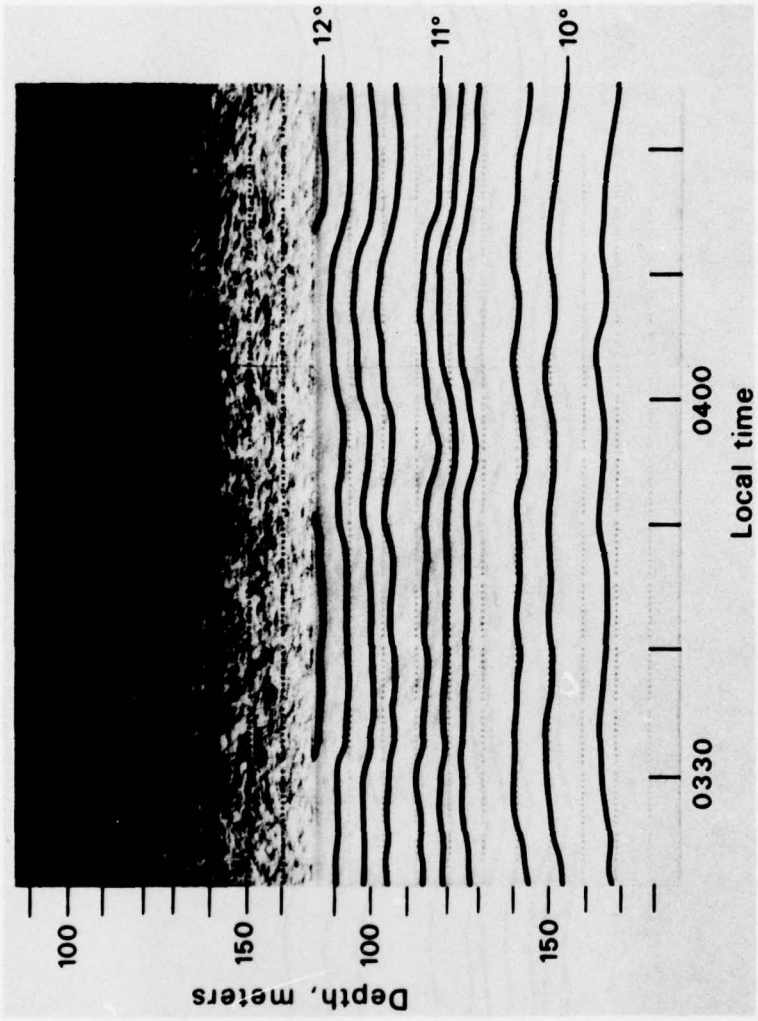

Figure 12f

DISTRIBUTION LIST

Chief of Naval Research
Department of the Navy
Arlington, Virginia 22217
- Code 200 (1)
- Code 222 (2)
- Code 1021P (1)
- Code 102OSC (1)
- Code 460 (1)
- Code 480 (1)
- Code 481 (1)
- Code 486 (1)

Director
Office of Naval Research
Branch Office
1030 East Green Street
Pasadena, California 91101 (1)

Commander
Naval Sea Systems Command
Washington, D.C. 20362
- Code 03E (1)
- Code 034 (1)
- Code 0342 (1)
- Code 036 (1)
- Code 06H1 (1)
- Code 06H2 (1)
- Code 09G3 (1)
- Code 92 (1)
- Code 662C14 (1)
- Code PMS 395-4 (1)
- Code 402 B (1)
- Code 03423 (Mr. Francis J. Romano) (1)

Commander
Naval Air Systems Command
Washington, D.C. 20361
- Code 370 (1)
- Code 264 (1)

Commander
Naval Electronics
Systems Command
Washington, D.C. 20360
- Code PME-124 (1)

Chief of Naval Material
Department of the Navy
Washington, D.C. 20360
- Code PM-4 (1)
- Code 034 (1)
- Code ASW121 (1)

Chief of Naval Operations
Department of the Navy
Washington, D.C. 20350
- Code Op 03 (1)
- Code Op 32 (1)
- Code Op 098 (1)
- Code Op 02 (1)
- Code Op 095 (1)
- Code Op 23 (1)
- Code Op 967 (1)

Commanding Officer
Naval Ocean Research &
Development Activity (NORDA)
National Space Technology Laboratories
Bay St. Louis, Mississippi 39529
- Code 100 (1)
- Code 460 (1)
- Code 500 (1)

Oceanographer of the Navy
The Hoffman Building
200 Stoval Street
Alexandria, Virginia 22332 (1)

Director Strategic Systems
Projects Office (PM-1)
Department of the Navy
Washington, D.C. 20360
- Code NSP-20 (1)

Director
Defense Research & Engineering
The Pentagon
Washington, D.C. 20301
- Assistant Director (Sea Warfare Systems) (1)

Assistant Secretary of the Navy
(Research & Development)
Department of the Navy
Washington, D.C. 20350 (1)

U.S. Naval Oceanographic Office
Washington, D.C. 20373
- Code 1640 (1)
- Code 3440 (1)

Commander Operational Test &
Evaluation Force
U.S. Naval Base
Norfolk, Virginia 23511 (1)

Commander, Submarine Force
U.S. Pacific Fleet
Fleet Post Office
San Francisco, California 96601 (1)

Commander
Submarine Group FIVE
Fleet Station Post Office
San Diego, California 92132 (1)

Commander
Third Fleet
U.S. Pacific Fleet, FPO
San Francisco, California 96610 (1)

Commander
Submarine Development Group ONE
Fleet Post Office
San Diego, California 92132 (1)

Commander
Submarine Development Group TWO
Naval Submarine Base-New London
Groton, Connecticut 06340 (1)

DISTRIBUTION LIST (Continued)

Commander, Surface Force
U.S. Atlantic Fleet
Norfolk, Virginia 23511 (1)

Commander, Surface Force
U.S. Pacific Fleet
San Diego, California 92155 (1)

Reprint Custodian
Department of Nautical Science
U.S. Merchant Marine Academy
Kings Point, New York 11024 (1)

Deputy Commander
Operational Test &
Evaluation Force, Pacific
U.S. Naval Air Station
San Diego, California 92135 (1)

Commander
Naval Ship Research &
Development Center
Bethesda, Maryland 20084 (1)

Naval Civil Engineering Laboratory
Port Hueneme, California 93041
Code L40 (1)
Code L42 (1)

Naval Facilities
Engineering Command
Washington, D.C. 20390
Code 03 (1)
Code 032C (1)

Commanding Officer
U.S. Naval Air Development Center
Warminster, Pennsylvania 18974 (1)

Commander
Naval Ocean Systems Center
San Diego, California 92152
Code 6700 (2)

Officer in Charge
Naval Ship Research & Development
Center
Annapolis, Maryland 21402 (1)

Commanding Officer, Naval
Coastal Systems Laboratory
Panama City, Florida 32401 (1)

Commander
Naval Surface Combat Systems Center
White Oak
Silver Spring, Maryland 20910 (1)

Director
U.S. Naval Research Laboratory
Washington, D.C. 20375
Code 2620 (1)
Code 2627 (1)
Code 8000 (1)
Code 8100 (1)

Commanding Officer
Naval Underwater Systems Center
Newport, Rhode Island 20844
Attn: John D'Albora (1)

Commanding Officer
Naval Underwater Systems Center
New London, Connecticut 06320
Code 900 (1)
Code 905 (1)
Code 910 (1)
Code 930 (1)
Code 960 (1)

Commanding Officer
Naval Training Equipment Center
Orlando, Florida 32813
Tech Library (1)

Chief Scientist
Navy Underwater Sound
Reference Division
U.S. Naval Research Laboratory
P.O. Box 8337
Orlando, Florida 32806 (1)

Superintendent
U.S. Naval Postgraduate School
Monterey, California 93940 (1)

Director
Defense Documentation Center
(TIMA), Cameron Station
5010 Duke Street
Alexandria, Virginia 22314 (12)

Executive Secretary
National Academy of Sciences
2101 Constitution Avenue, N.W.
Washington, D.C. 20418 (1)

Supreme Allied Commander
U.S. Atlantic Fleet
ASW Research Center
APO
New York, New York 09019
Via: ONR 210
CNO OPO92D1
Secretariat of Military
Information Control
Committee (1)

National Oceanic & Atmospheric Administration
6001 Executive Boulevard
Rockville, Maryland 20852 (1)

Director of Naval Warfare Analysis
Institute of Naval Studies
1401 Wilson Boulevard
Arlington, Virginia 22209 (1)

Institute for Defense Analyses
400 Army-Navy Drive
Arlington, Virginia 22202 (1)

Director
Woods Hole Oceanographic Institution
Woods Hole, Massachusetts 02543 (1)

Meteorological & Geo-Astrophysical Abstracts
301 E. Capitol Street
Washington, D.C. 20003 (1)

Director
Applied Physics Laboratory
University of Washington
1013 East 40th Street
Seattle, Washington 98105 (1)

National Science Foundation
Washington, D.C. 20550 (2)

Director
Lamont-Doherty Geological Observatory
Torrey Cliff
Palisades, New York 10964 (1)

Director
College of Engineering
Department of Ocean Engineering
Florida Atlantic University
Boca Raton, Florida 33431 (1)

Director
Attn: Dr. J. Robert Moore
Institute of Marine Science
University of Alaska
Fairbanks, Alaska 99701 (1)

Director
Applied Research Laboratory
Pennsylvania State University
P.O. Box 30
State College, Pennsylvania 16802 (1)

Director
University of Texas
Applied Research Laboratory
P.O. Box 8029
Austin, Texas 78712 (1)

STOIAC
Battelle Columbus Laboratories
505 King Avenue
Columbus, Ohio 43201 (1)

Director
Institute of Ocean Science & Engineering
Catholic University of America
Washington, D.C. 20017 (1)

Director
Marine Research Laboratories
c/o Marine Studies Center
University of Wisconsin
Madison, Wisconsin 53706 (1)

Office of Naval Research
Resident Representative
c/o University of California, San Diego
La Jolla, California 92093 (1)

University of California, San Diego
MPL Branch Office
La Jolla, California 92093 (5)